



# Transportation Research Division



## **Technical Report 15-10**

*Long Term Monitoring of Carbon Composite Strands in the Penobscot- Narrows Bridge*

*Final Report – June 2015*

Technical Report Documentation Page

1. Report No. ME 15-10		2.		3. Recipient's Accession No.	
4. Title and Subtitle Long Term Monitoring of Carbon Fiber Composite Strands in the Penobscot Narrows Bridge				5. Report Date June 2015	
				6.	
7. Author(s) Keith Berube Roberto Lopez-Anido Ph.D, P.E.				8. Performing Organization Report No. AEWC Report Number 15-1098	
9. Performing Organization Name and Address University of Maine – Advanced Structures and Composites Center				10. Project/Task/Work Unit No.	
				11. Contract © or Grant (G) No.	
12. Sponsoring Organization Name and Address Maine Department of Transportation				13. Type of Report and Period Covered	
				14. Sponsoring Agency Code	
15. Supplementary Notes					
16. Abstract (Limit 200 words)					
<p>The Penobscot-Narrows Bridge was constructed between May 2003 and December 2006. The bridge is a cable-stayed design with twin pylons and a 2,120-foot span. This cable-stayed bridge features a cradle stay system that allows for each cable strand in the stay to span between the main-span bridge deck anchorage, through the pylon, and then down to the back-span bridge deck anchorage. In each pylon, twenty stays run through individual cradle systems with each stay enclosed in a high-density polyethylene (HDPE) sheathing extending from the pylon to the bridge deck.</p> <p>The unique design features of the cable support and anchorage systems used in the Penobscot-Narrows Bridge not only permit the replacement of each cable strand, but also present engineers with the opportunity to test a variety of cable designs and materials for their longevity and performance in order to better serve the entire bridge industry. The engineers at MaineDOT recognized this, so in June 2007, two steel strands were removed from each stay, at stay numbers 2, 10 and 17 of the Prospect side pylon, while concurrently installing two carbon-fiber composite cables (CFCC) in their place.</p> <p>This report provides data and analysis of the CFCC cables from the installed structural monitoring system and makes recommendations for long term monitoring of the cables.</p> <p>A previous report documented the CFCC installation, instrumentation and initial data analysis.</p>					
17. Document Analysis/Descriptors Cable stayed bridge, carbon fiber composite cables, structural monitoring				18. Availability Statement	
19. Security Class (this report)		20. Security Class (this page)		21. No. of Pages 48	22. Price

# Final Technical Report

## Long-Term Monitoring of Carbon Composite Strands in the Penobscot-Narrows Bridge

Prepared for:  
Dale Peabody, Maine Department of Transportation

Prepared by:  
Keith A. Berube and Roberto A. Lopez-Anido  
Advanced Structures and Composites Center  
University of Maine

Report Number 15-1098

June 2, 2015

*An ISO 17025 accredited testing laboratory  
Accredited by international Accreditation Service*



## **Introduction**

The Penobscot-Narrows Bridge was constructed between May 2003 and December 2006. The bridge crosses the Penobscot River between Prospect and Verona, Maine in the proximity of Fort Knox. The team responsible for the design of the Penobscot-Narrows Bridge included the MaineDOT, the Federal Highway Administration and Figg Bridge Engineers, Inc. The bridge is a cable-stayed design with twin pylons and a 2,120-foot span. This cable-stayed bridge features a cradle stay system, designed by Figg Bridge Engineers, Inc. This cradle system allows for each cable strand in the stay to span between the main-span bridge deck anchorage, through the pylon, and then down to the back-span bridge deck anchorage. In each pylon, twenty stays run through individual cradle systems with each stay enclosed in a high-density polyethylene (HDPE) sheathing extending from the pylon to the bridge deck. The HDPE sheathing is designed to provide the ability to be ventilated with forced dry air to prevent corrosion of the cables.

The unique design features of the cable support and anchorage systems used in the Penobscot-Narrows Bridge not only permit the replacement of each cable strand, but also present engineers with the opportunity to test a variety of cable designs and materials for their longevity and performance in order to better serve the entire bridge industry. The engineers at MaineDOT recognized this, so in June 2007, two steel strands were removed from each stay, at stay numbers 2, 10 and 17 of the Prospect side pylon, while concurrently installing two carbon-fiber composite cables (CFCC) in their place. Figure 1 illustrates the locations of the stays containing CFCC strands.

The CFCC strands and anchors were supplied by Tokyo Rope, with technical assistance from Lawrence Technological University (LTU), Southfield, Michigan. The CFCC strands were successfully installed by the same contracting team that built the bridge, Cianbro/Reed & Reed JV. Inspection and technical assistance during the carbon fiber strand installation was provided by the MaineDOT, Figg Bridge Engineers, LTU, Tokyo Rope and the University of Maine (UMaine). A technical report was submitted to MaineDOT (Lopez-Anido et al. 2009).

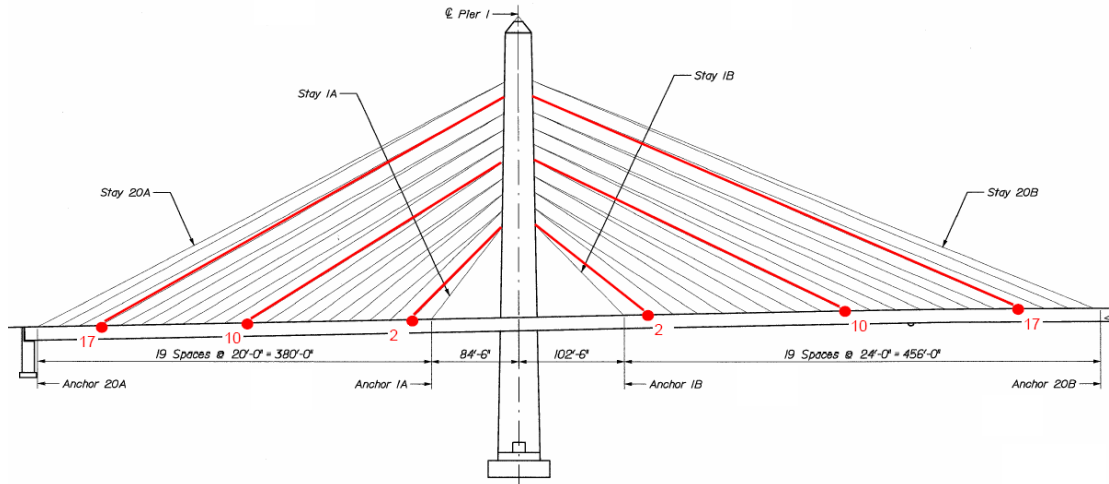


**Figure 1. Stays with CFCC strands in the north pylon of the Penobscot Narrows bridge.**

### Structural Monitoring System

A system capable of monitoring the load and strain in the CFCC strands was implemented during the summer of 2007. The instrumentation system was developed and designed by a team comprised of the University of Maine, MaineDOT, LTU, Dywidag-Systems International (DSI), Construction Technology Laboratories, Inc. (CTL Group), Skokie, IL, and Figg Bridge Engineers. The instrumentation installed at the Penobscot-Narrows Bridge site includes five different sensor components and two interfaces (Berube et al. 2008a).

The sensor components include linear variable differential transformers (LVDTs), fiber-optic strain (FOS) sensors, temperature sensors, load-cells, and DYNA-Force Elasto-Magnetic Sensors. The DYNA-Force sensors are mounted to three steel strands at every stay anchorage and can be monitored locally with a Power-Stress Unit provided by DSI which displays the load in the steel cables. The CFCC strand monitoring system implemented requires local monitoring of the load-cells, FOS sensors, temperature sensors, and LVDTs.

The interfaces include the junction box, mounted to the concrete stay anchor block, and the egress box, mounted on the stay end-cap. The egress box allows the sensors to be disconnected for stay anchorage maintenance without compromising the integrity of the end-cap, or removal of the sensors from their mounted positions.

The instrumentation described was installed at stay anchor locations 2, 10 and 17, and provided MaineDOT with valuable information about the conditions of the steel and CFCC strands present in the stay-cable assemblies.

The instrumentation allows the monitoring of:

- 1) Load in the steel strands
- 2) Strain and load in the CFCC strands
- 3) Temperature inside the stay-cable anchorage end-cap
- 4) Axial deformation of the CFCC strand anchorage-chair
- 5) Ambient temperature at the bridge site.

An external temperature sensor was used during periodic monitoring sessions to provide the ambient temperature at the bridge site. The ambient temperature is a crucial measurement in order to correlate load fluctuations in the CFCC strands to temperature fluctuations. The load fluctuations in the CFCC strands may be sizable due to the ratio of the number of steel to CFCC strands and the mismatch in coefficient of the thermal expansion (CTE) of the steel and CFCC strands. The CTE for the steel strand is almost 20 times larger than the CTE of the CFCC strand.

## **Installed Instrumentation and Sensors**

### **Load-Cells**

The 40-kip load-cells were designed, fabricated, and calibrated by CTL. The load-cells incorporated an open-hole design, which allowed them to be mounted around the CFCC strand anchor sleeve and loaded in compression between the top of the anchorage-chair and a nut applied to the threaded CFCC strand anchor sleeve during the CFCC strand tensioning operation. The load-cells were intended to be monitored at a datalogger located at the south side of the north pylon inside the bridge deck. A current-loop system was implemented for this purpose. (*Note: The CTL logging system stopped working in 2009*)

### **Fiber-Optic Strain Sensors**

FOS sensors were utilized to monitor the strain in the CFCC strand, since they can provide an absolute measure of strain. The FOS sensors were incorporated into a composite split sleeve design, which allowed them to be readily attached to the CFCC strand. The FOS sensor sleeve measures the absolute strain in the CFCC strand it is attached to through the two embedded FOS sensors in the sleeve. The sleeves were fabricated and calibrated in the laboratory and then mounted to the CFCC strands after the CFCC strands were tensioned.

### **LVDTs**

An LVDT system was employed to monitor the CFCC strand anchorage-chair deformations. The system consists of an LVDT mounted near the top of each anchorage-chair leg with an extension rod running the length of each chair leg and attached near its base. The LVDT measures the axial deformation of the chair due to both fluctuations in

CFCC strand force and thermal expansions in the chair material due to the change in ambient temperature at the anchorage location.

### **Temperature Sensors**

The temperature sensors were mounted to the anchorage-chair in the end-cap to monitor temperature at the anchorage location. The temperature at this location is needed to account for the temperature effects on the installed instrumentation and to compute the CTE effects on the CFCC strand anchorage-chair and LVDT extension rods. They were fabricated in the laboratory using precision integrated-circuit temperature sensors, which provide a voltage output proportional to the temperature in degrees Fahrenheit. The sensors were calibrated in the laboratory before installation at the bridge site.

### **Egress Box**

The sensor egress box is mounted on the galvanized steel end-cap at each CFCC strand anchorage location. The wire leads of the FOS sensors, temperature sensors, LVDTs and load-cells are wired into the egress box such that they can be disconnected from the end-cap to allow for its removal.

### **Junction Box**

The junction box provides the external interface for both powering the sensors and acquiring the sensor data during local monitoring. The junction box is mounted on the face of the concrete stay anchor block at each CFCC strand anchorage location. The sensor leads are connected from the junction box to the egress box through a 1.5-in diameter flexible conduit.

### **Objectives**

The objectives of the proposed research project are:

- 1) Verification of the installed instrumentation and sensor systems. The verification includes checking that the sensors and connections are operational and correlating the fiber optic sensor strains, displacement transducer and load-cell measurements to the baseline values established in 2007.
- 2) Continuous measurement of installed instrumentation and sensor systems. This will demonstrate that the installed instrumentation system can provide a continuous record of the carbon composite strand response over an extended period of time (for example, one week). This will also serve to verify that the fiber optic sensor strains and displacement transducer measurements correlate to the load-cell outputs.

- 3) Feasibility study for connecting the instrumentation to the web based dry air monitoring system. This will identify what instruments and sensors can be connected online to the existing dry air monitoring system.

## Scope of Work

### Task 1 – Verification of the Installed Instrumentation and Sensor Systems

The verification included checking that the sensor systems and connections are operational. The procedure for verifying the sensor systems was to conduct onsite monitoring at each anchorage location. The data acquisition components required were:

- 1) DaqBook 2005 with DBK1– 16-bit A/D DAQ system with 16-channel BNC module.
- 2) UMI-8 – FOS monitoring unit.
- 3)  $\pm 15V$  DC Power supply, which provides power to the sensors installed at the bridge site.
- 4) P-3500 Strain Indicating Unit, which is the load-cell monitoring system.
- 5) Laptop computer.
- 6) DYNA-Force EM Monitoring Unit.

An image of the data acquisition during local monitoring at the anchorage location is presented in Figure 2 and a schematic is depicted in Figure 3.

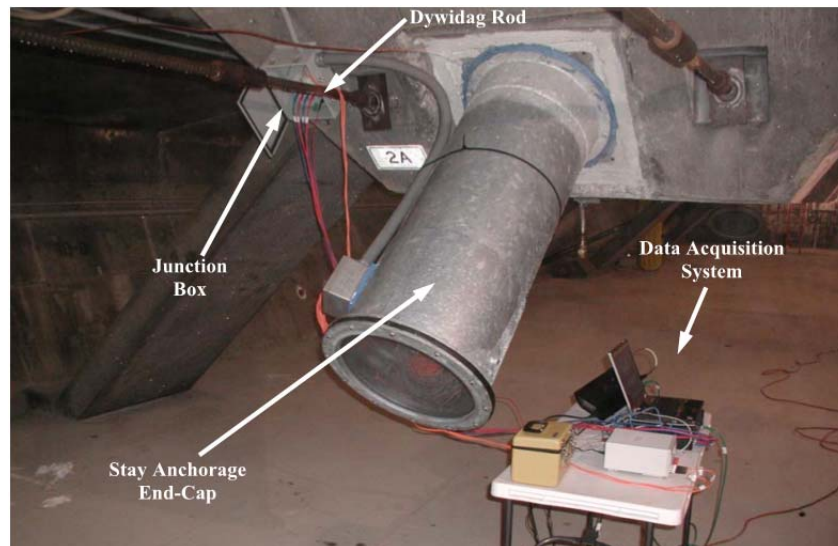


**Figure 2. Data acquisition set up at stay anchorage location.**

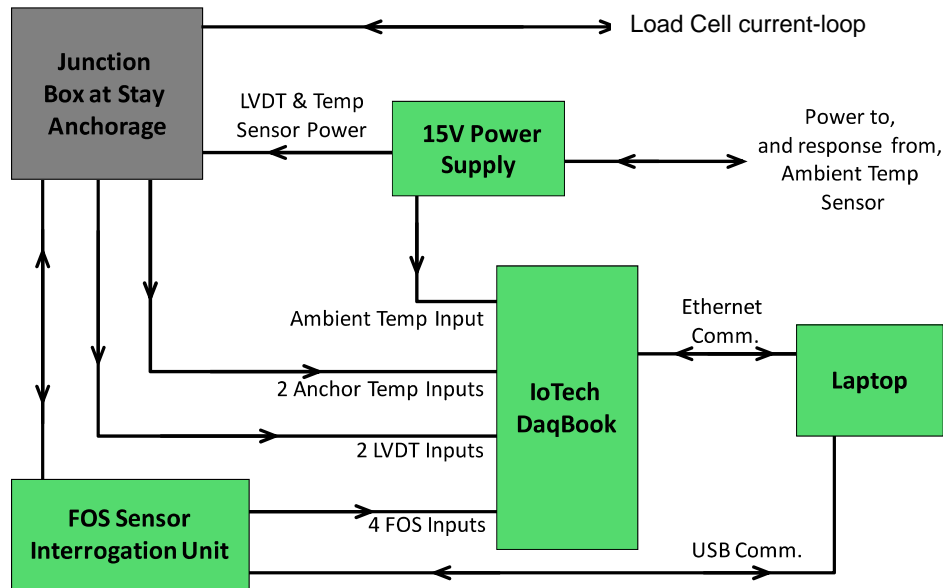


**Figure 3. Schematic of data acquisition system.**

The operational status of the sensor system was verified at each of the six stay anchorage locations during a trip to the bridge site in late November 2012. While there were the expected minor variations in LVDT and fiber optic sensor data, all of the CFCC strand forces, anchorage-chair deflection data, and FOS sensor data were comparable to the data previously recorded since the system was installed in late June 2007.

## **Task 2 – Continuous Measurement of Installed Instrumentation and Sensor Systems**

Continuous monitoring was conducted at stay location 10B for a period of one week in March 2008 (Berube et al. 2008b). This procedure was repeated at each of the six stay anchorage locations during the current project. The intent was to demonstrate that the installed instrumentation system can provide a continuous record of the carbon composite strand response over an extended period of time (e.g. one week). This also served as a means to verify that the fiber optic sensor strains and displacement transducer measurements correlated to the load-cell outputs.

Continuous monitoring data was recorded at each of the six stay locations for a period of approximately one week and was obtained twice during the year; February 7 to March 29, 2013 and September 4 to October 9, 2013. This provided two sets of week-long data at each of the six locations. It is worth noting that the 10B dataset recorded in March 2013 lasted for a 14-day period, due to a scheduling conflict.

A summary of the CFCC load-cell data for the two monitoring time periods is presented in Table 1. The table includes the change in external temperature experienced during the monitoring period along with the fluctuation in CFCC force due to this change in external temperature. The relationships between temperature and cable response are affected by

the differences between coefficients of thermal expansion and the relative axial stiffness of the CFCC and steel strands at each stay anchor location. The axial stiffness is the product of the elastic modulus and the cross-sectional area of all the strands in one stay.

The table also includes the original CFCC load-cell readings that were recorded during the CFCC installation in June 2007. Most of the loads are lower than what they were when originally installed, which is as expected, since they were installed during warm weather when the steel cables were longer due to their thermal expansion.

**Table 1. CFCC load-cell results for continuous monitoring during 2013.**

Stay	Time Period	External Temperature		CFCC Force Range (lb)			
		Range (°F)		Left Cable		Right Cable	
#	start to end-date	Low	High	Low	High	Low	High
	<i>Installation 06/2007</i>		--	<b>26,060</b>		<b>25,770</b>	
<b>2A</b>	02/21 to 03/01/13	20	34	26,020	26,317	24,233	24,615
	09/18 to 09/25/13	45	72	27,066	27,635	25,263	25,916
	<i>Installation 06/2007</i>		--	<b>22,490</b>		<b>22,460</b>	
<b>2B</b>	03/01 to 03/08/13	28	39	21,479	21,777	20,859	21,128
	10/02 to 10/09/13	41	76	21,777	22,635	21,590	22,340
	<i>Installation 06/2007</i>		--	<b>20,080</b>		<b>19,980</b>	
<b>10A</b>	02/07 to 02/14/13	13	42	18,552	19,164	18,157	18,796
	09/11 to 09/18/13	40	72	19,461	20,208	19,168	19,951
	<i>Installation 06/2007</i>		--	<b>20,970</b>		<b>21,050</b>	
<b>10B</b>	03/08 to 03/22/13	12	47	18,513	19,511	19,267	20,193
	09/11 to 09/18/13	40	72	19,483	20,457	19,756	20,771
	<i>Installation 06/2007</i>		--	<b>20,760</b>		<b>20,950</b>	
<b>17A</b>	02/07 to 02/14/13	3	41	18,583	19,481	18,651	19,564
	09/04 to 09/11/13	45	77	20,524	20,958	20,074	20,862
	<i>Installation 06/2007</i>		--	<b>20,810</b>		<b>20,250</b>	
<b>17B</b>	03/22 to 03/29/13	24	42	19,329	19,781	18,900	19,365
	09/04 to 09/11/13	45	77	19,850	20,966	19,305	20,467

Five series of plots of the continuous monitoring data were created to show the sensor response to changes in external temperature and to correlate response between CFCC force and other sensor types. The five different types of plots are as follows:

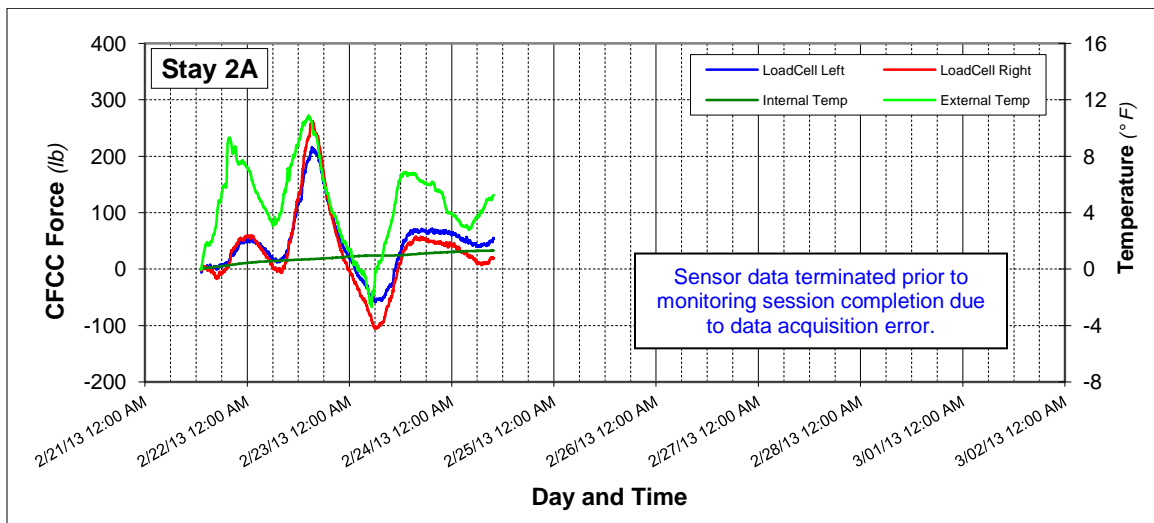
1. CFCC force compared to external temperature
2. Fiber-optic sensor strain compared to external temperature
3. LVDT Anchorage-chair deflection compared to external temperature
4. CFCC force compared to Fiber-optic sensor strain
5. CFCC force compared to LVDT Anchorage-chair deflection

End-cap internal temperature is also included in plot types 1-3.

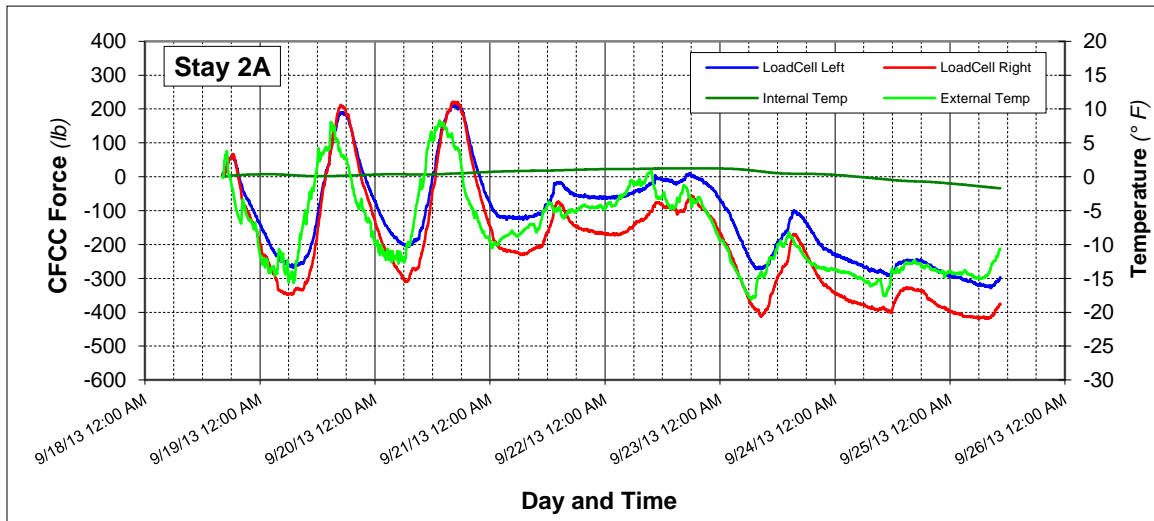
All sensor data are plotted as a change in signal response relative to the start of the data acquisition period. (i.e. All signals start at zero during the start of the cycle.) The relative signal method was chosen as a means to provide clarity in the response comparison between sensors due to differences in the magnitudes of the various sensor outputs.

### 1. CFCC Force Compared to External Temperature

Plots of the CFCC force data from the load-cells for each of the six stay locations during the two monitoring periods are presented in Figures 4-9. The CFCC load-cell data exhibit the same trend as the external temperature data with a slight lag in response time. This is due to the time it takes for the steel cables and CFCC strand to equilibrate to the surrounding temperature. The degree of lag appears to be affected by the gradient of the temperature change in the surrounding environment.

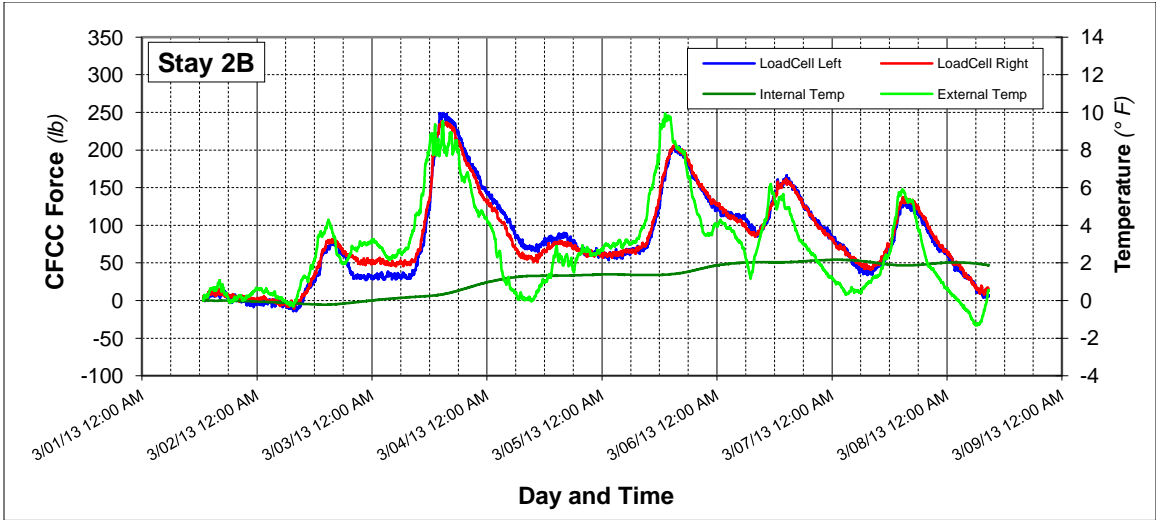


a)

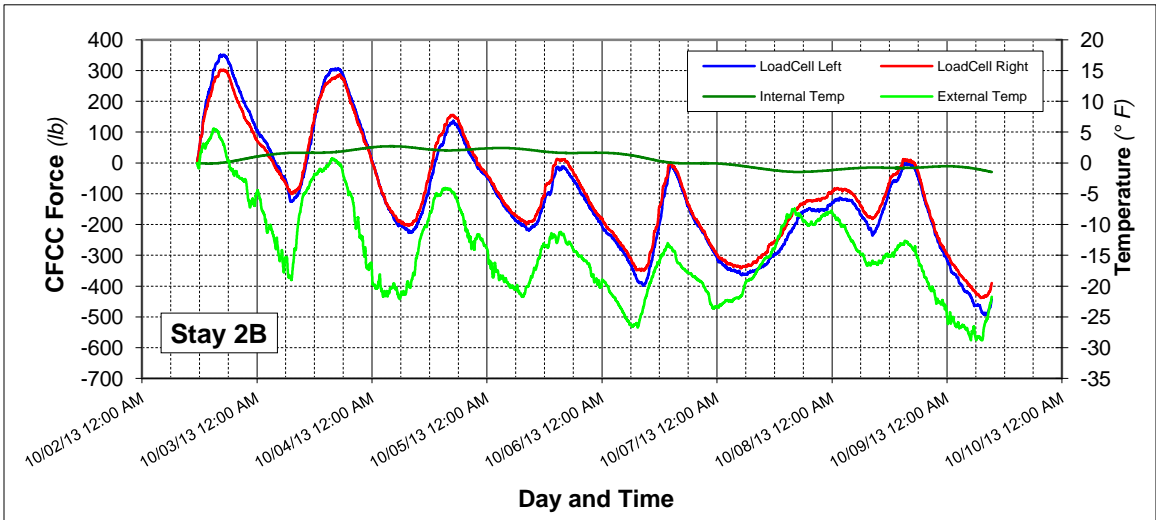


b)

**Figure 4. CFCC relative-force at Stay 2A during the continuous monitoring period in a) February 2013, and b) September 2013.**

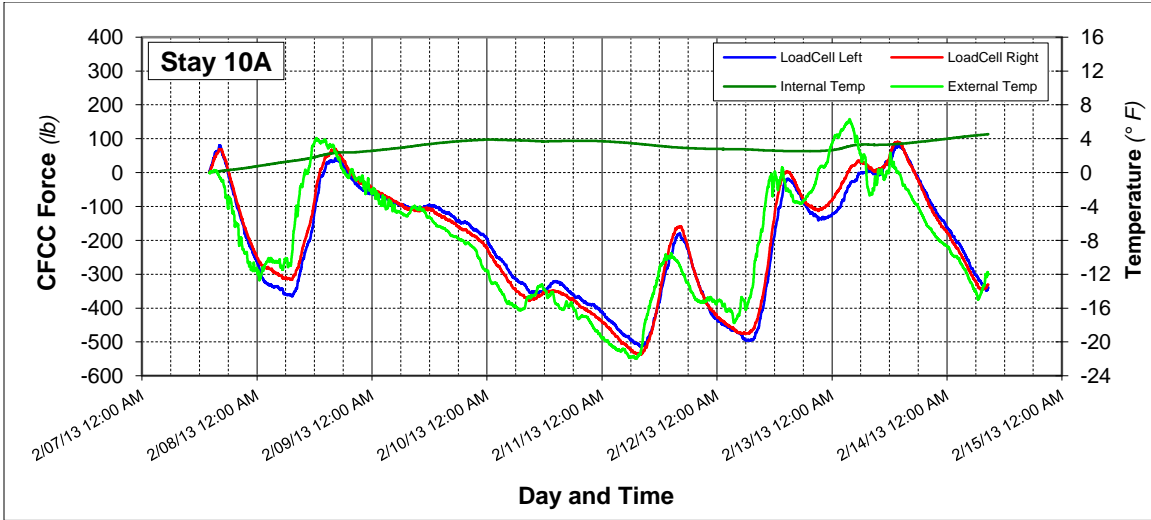


a)

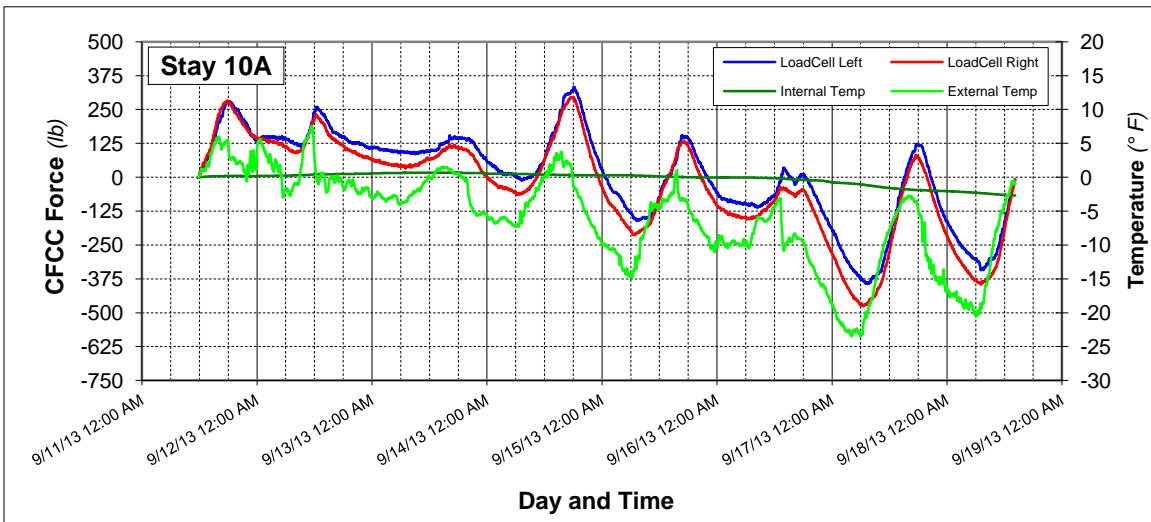


b)

**Figure 5. CFCC relative-force at Stay 2B during the continuous monitoring period in a) March 2013, and b) October 2013.**

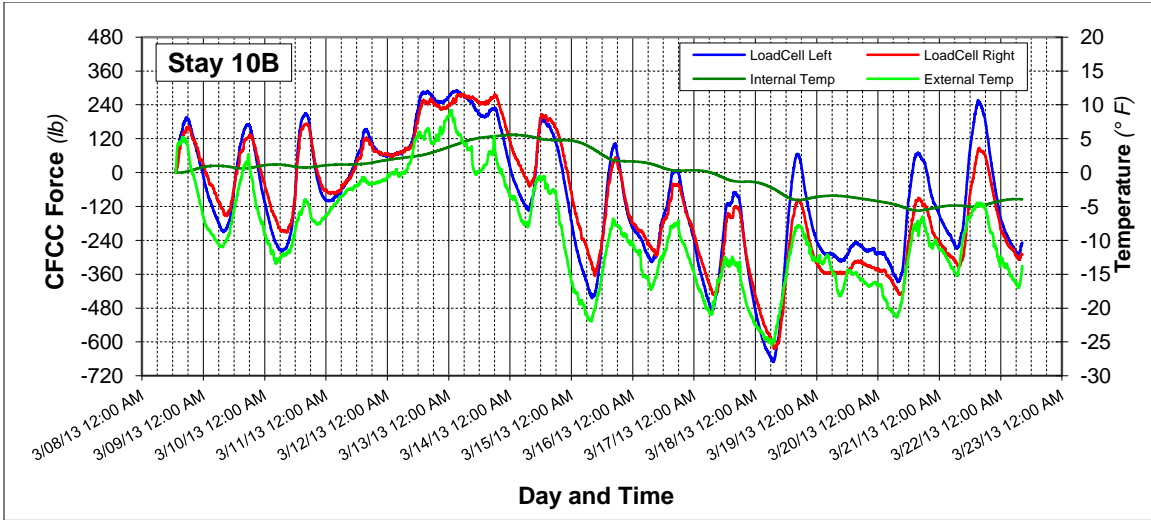


a)

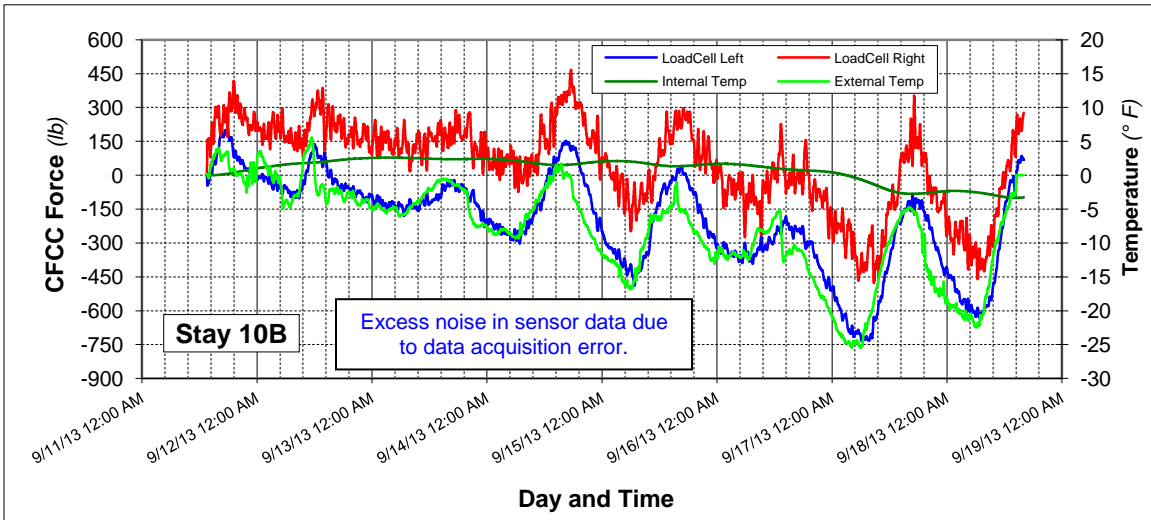


b)

**Figure 6. CFCC relative-force at Stay 10A during the continuous monitoring period in a) February 2013, and b) September 2013.**

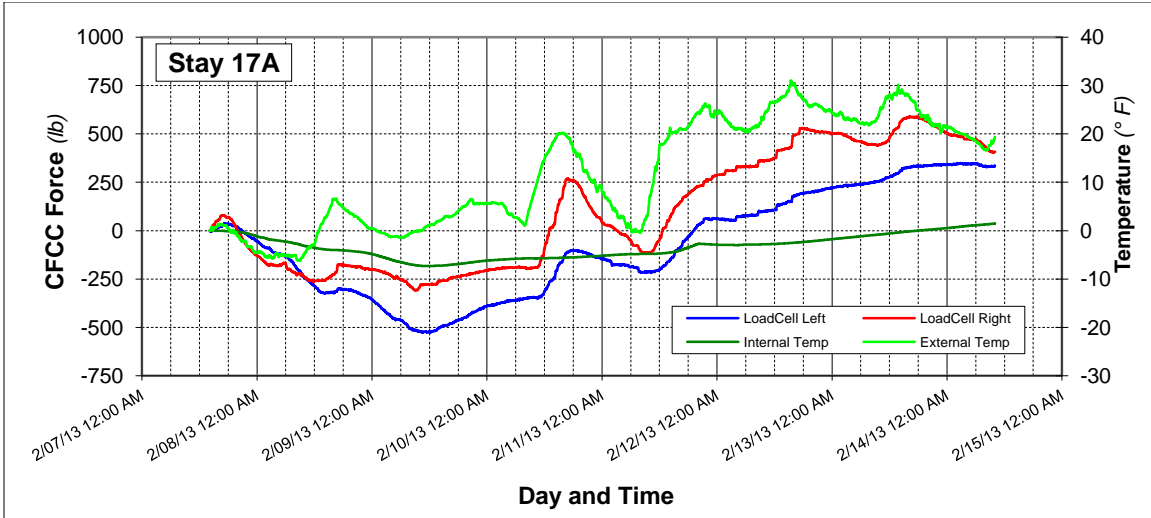


a)

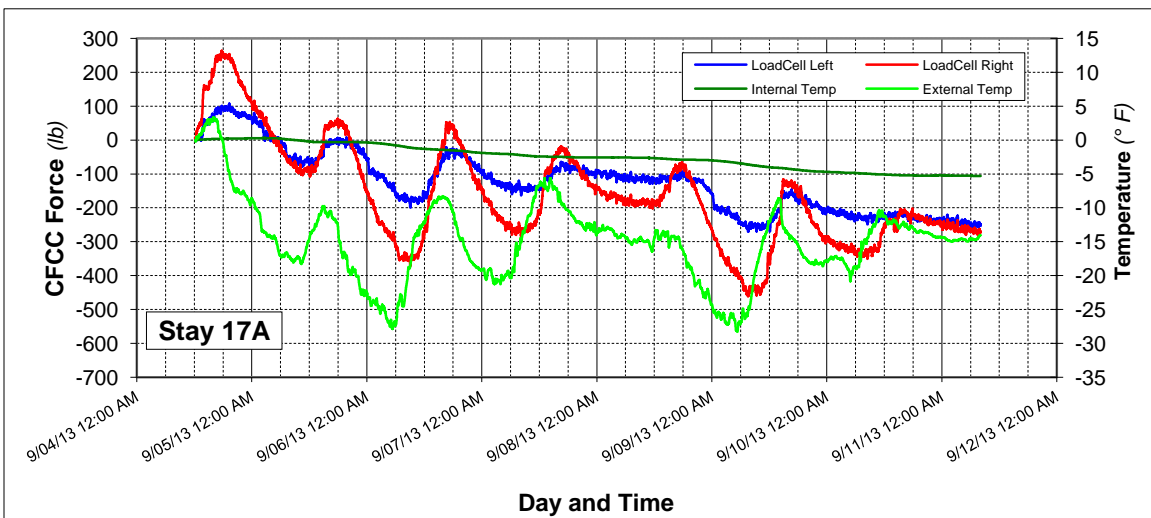


b)

**Figure 7. CFCC relative-force at Stay 10B during the continuous monitoring period in a) March 2013, and b) September 2013.**

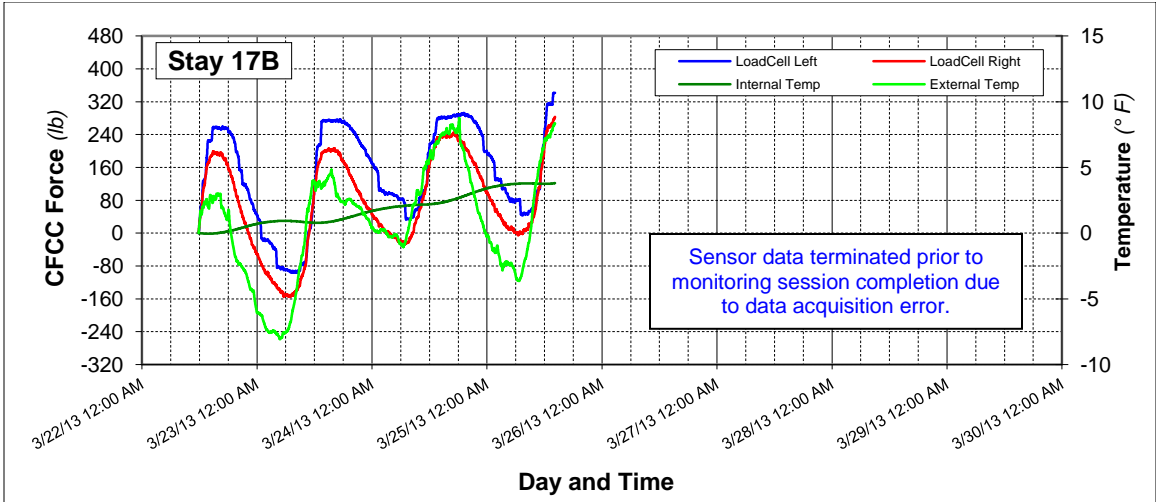


a)

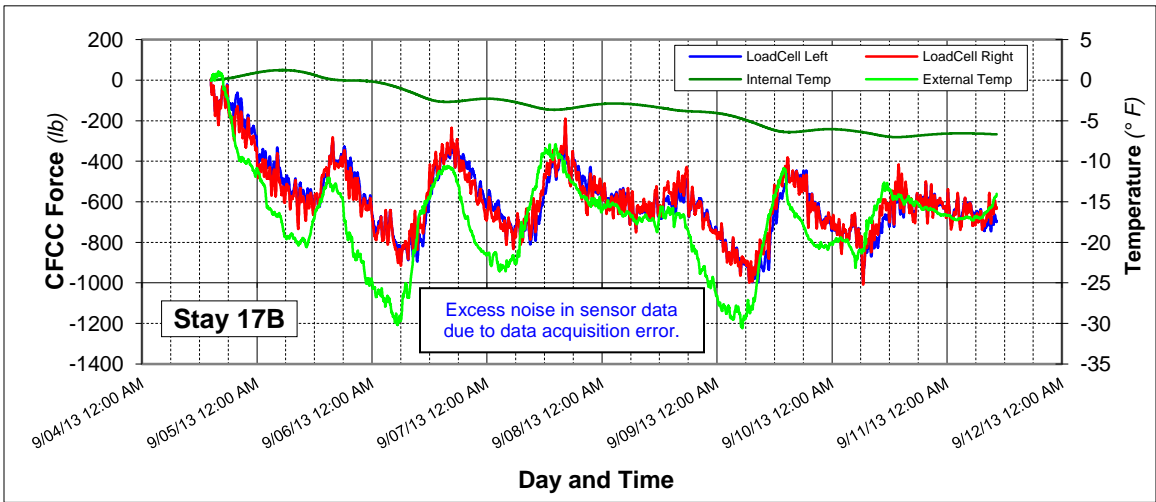


b)

**Figure 8. CFCC relative-force at Stay 17A during the continuous monitoring period in a) February 2013, and b) September 2013.**



a)

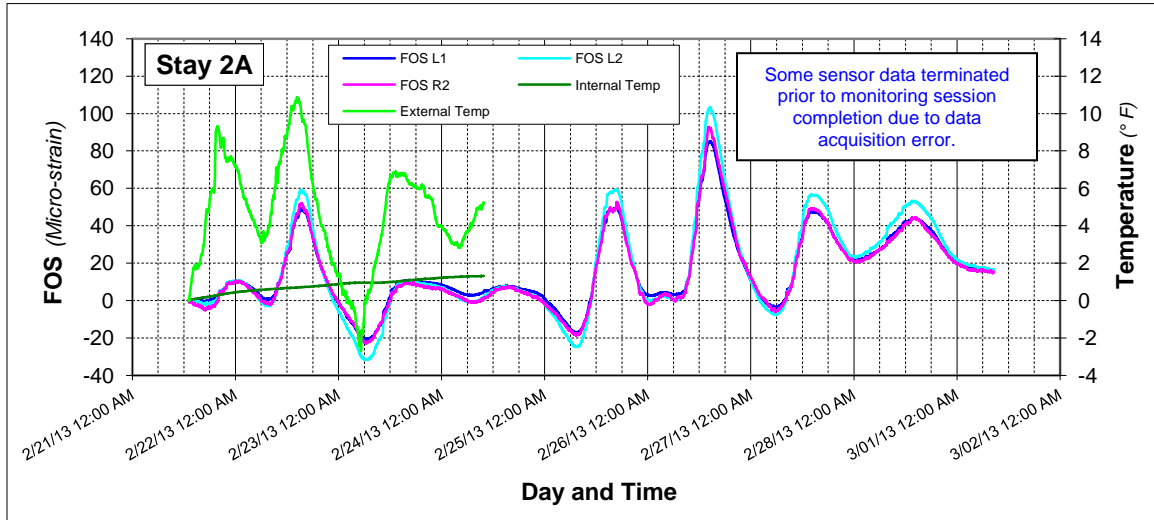


b)

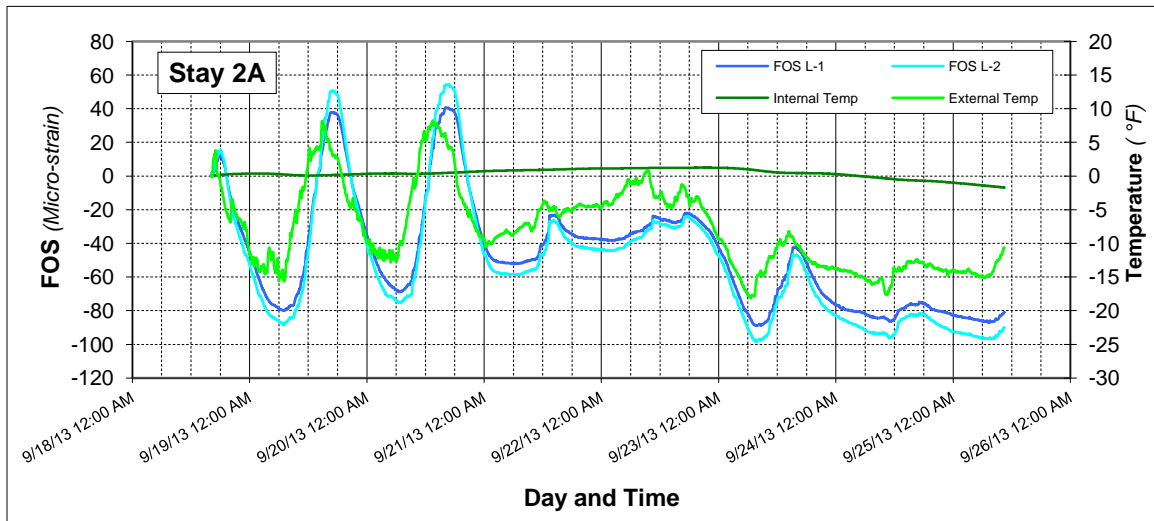
**Figure 9. CFCC relative-force at Stay 17B during the continuous monitoring period in a) March 2013, and b) September 2013.**

## 2. Fiber-Optic Sensor Strain Compared to External Temperature

Plots of the strain data from the FOS sensors for each of the six stay locations during the two monitoring periods are presented in Figures 10-15. Similar to the CFCC load-cell data, the FOS sensor data exhibit the same trend as the external temperature data with a slight lag in response time.

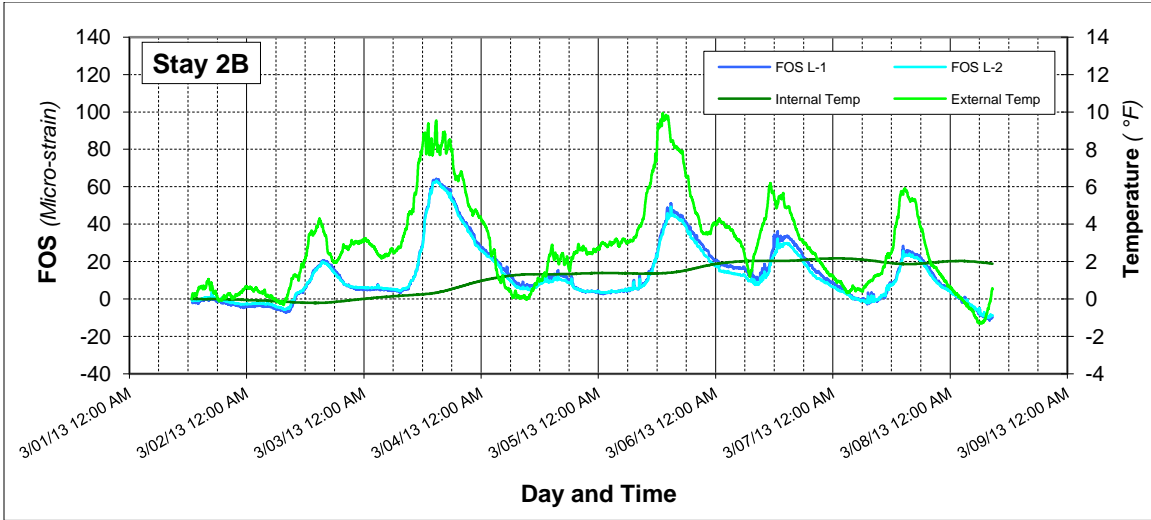


a)

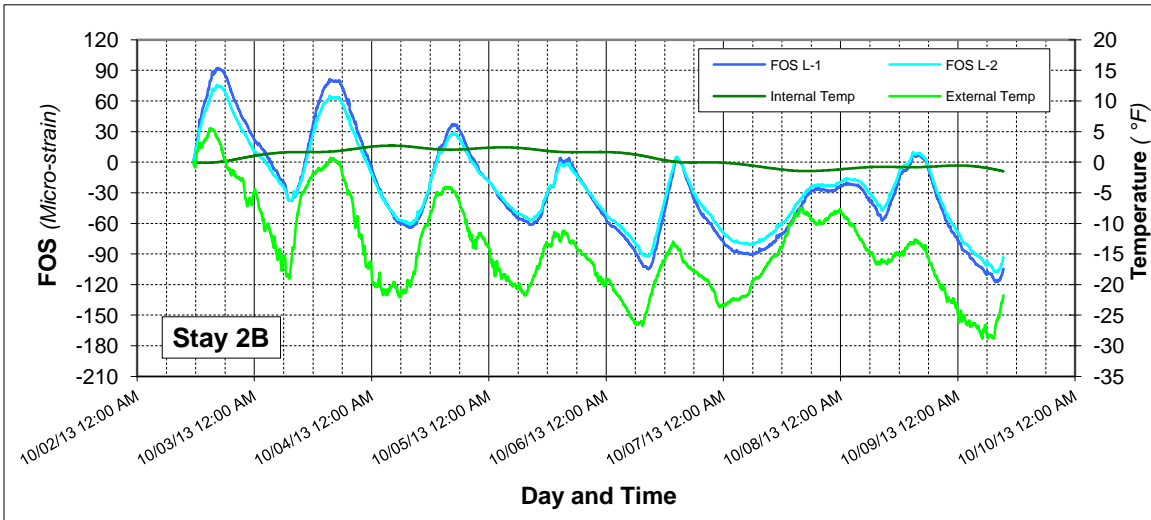


b)

**Figure 10. Fiber optic sensor relative-strain at Stay 2A during the continuous monitoring period in a) February 2013, and b) September 2013.**



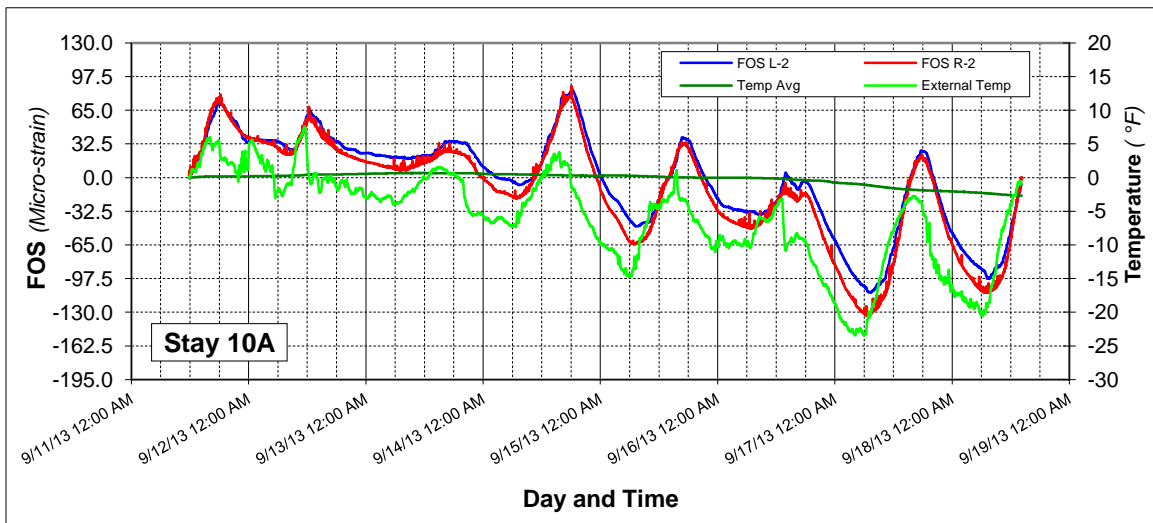
a)



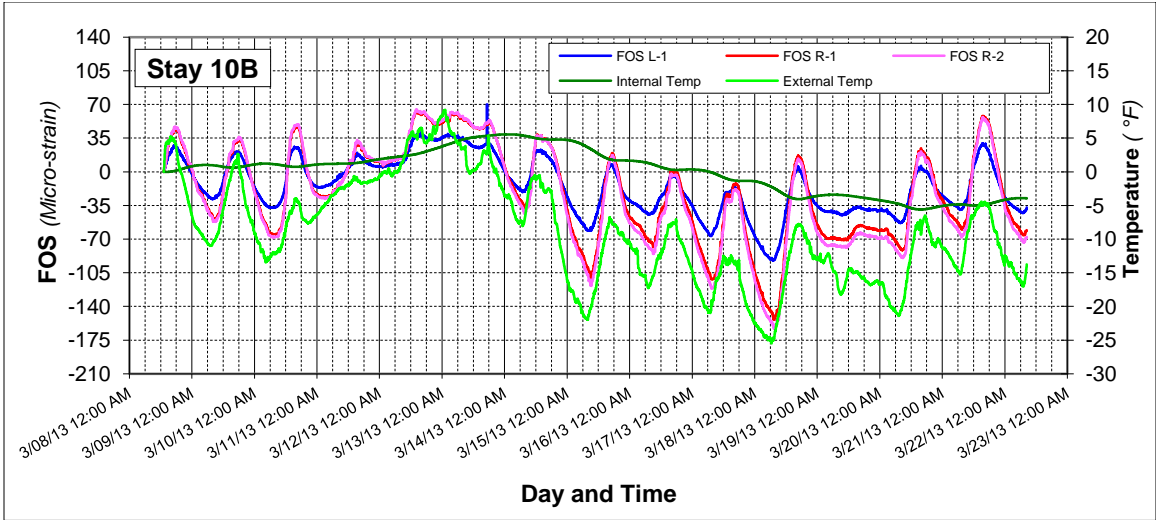
b)

**Figure 11. Fiber optic sensor relative-strain at Stay 2B during the continuous monitoring period in a) March 2013, and b) October 2013.**

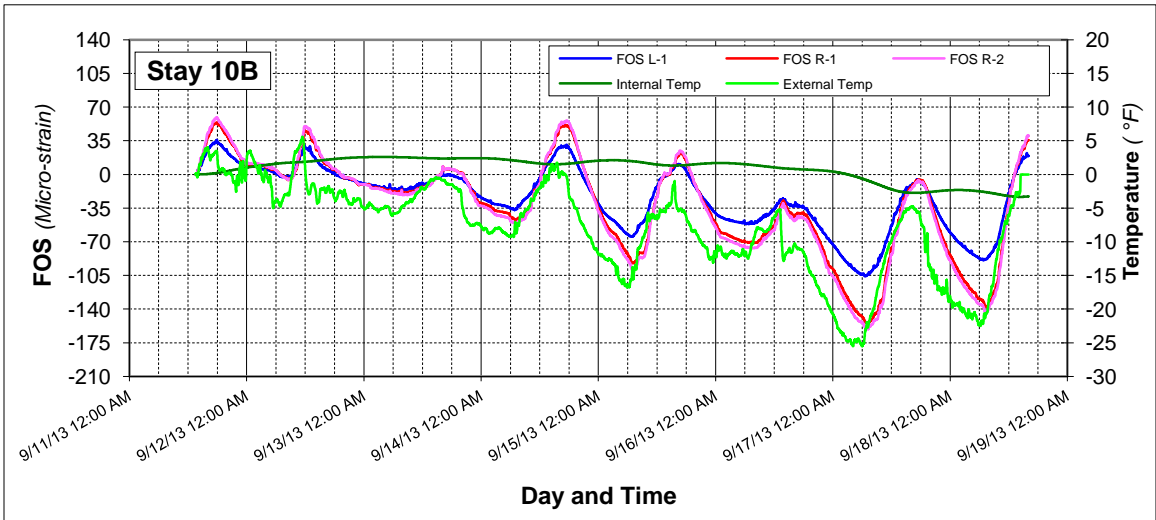
a) NO FIBER OPTIC SENSOR DATA AVAILABLE FOR THIS PERIOD DUE TO DATA ACQUISITION ERROR.



b) **Figure 12. Fiber optic sensor relative-strain at Stay 10A during the continuous monitoring period in a) March 2013, and b) September 2013.**

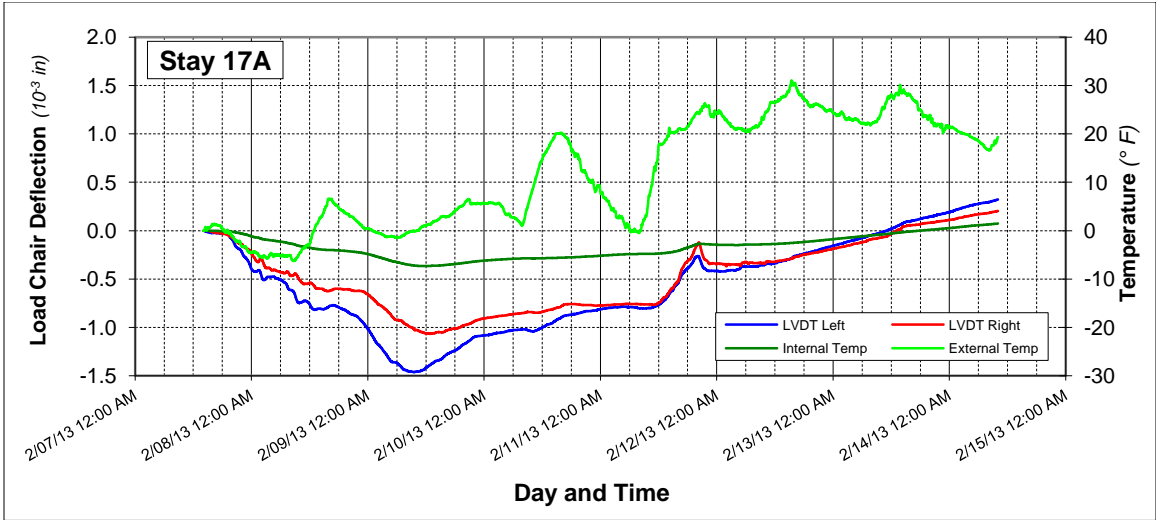


a)

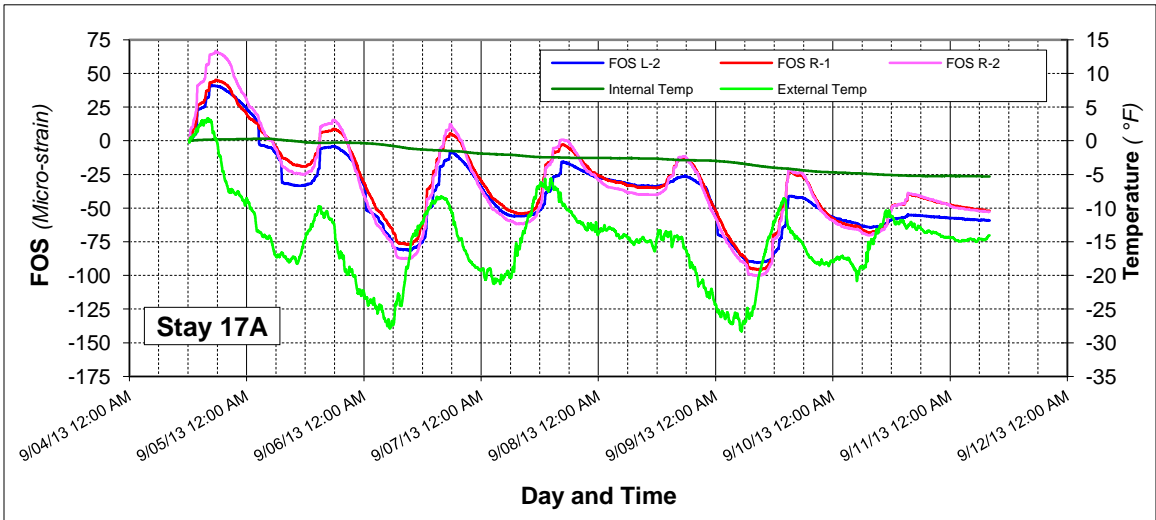


b)

**Figure 13. Fiber optic sensor relative-strain at Stay 10B during the continuous monitoring period in a) March 2013, and b) September 2013.**

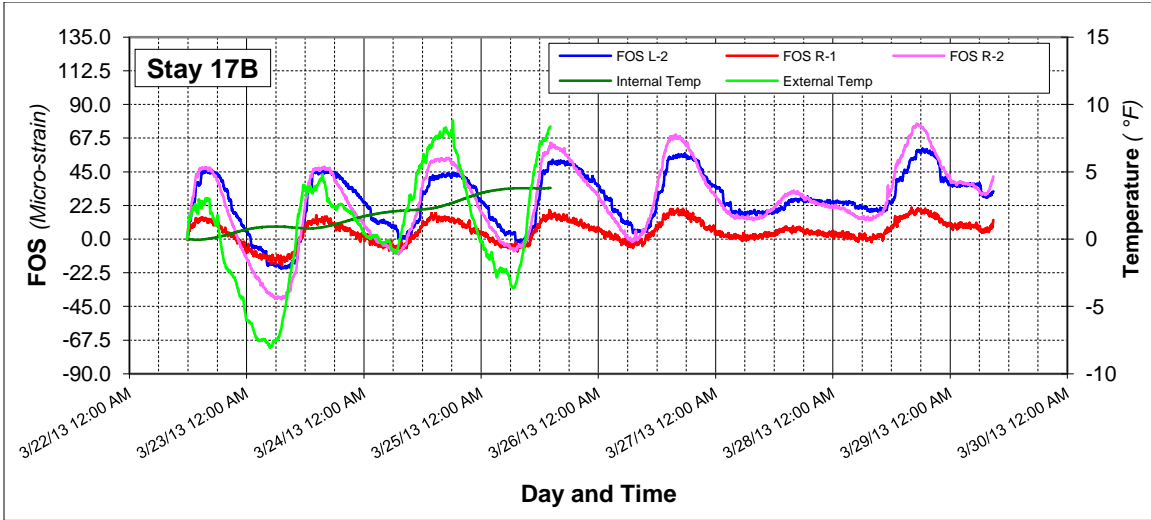


a)

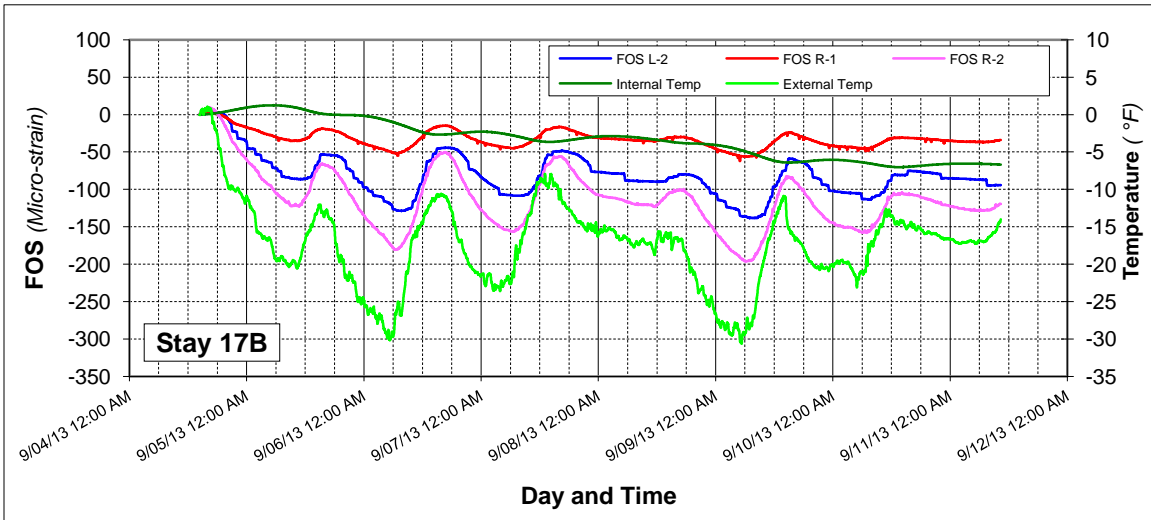


b)

**Figure 14. Fiber optic sensor relative-strain at Stay 17A during the continuous monitoring period in a) February 2013, and b) September 2013.**



a)

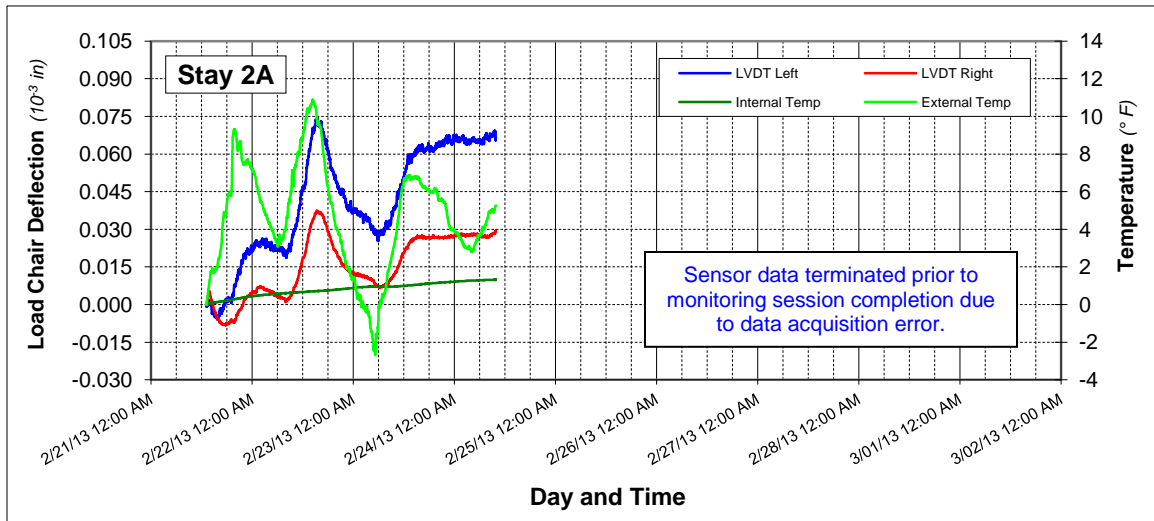


b)

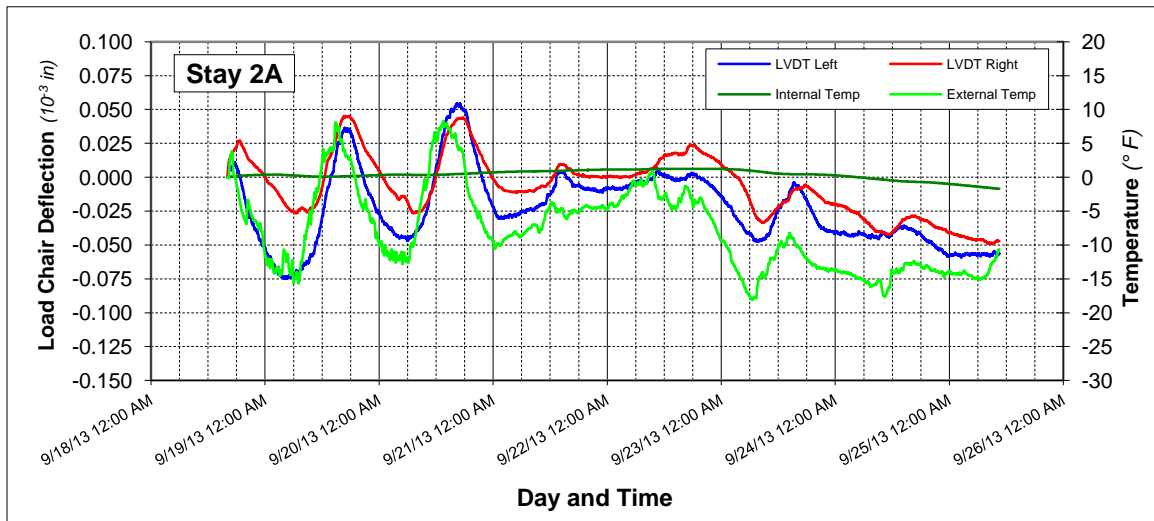
**Figure 15. Fiber optic sensor relative-strain at Stay 17B during the continuous monitoring period in a) March 2013, and b) September 2013.**

### 3. LVDT Anchorage-Chair Deflection Compared to External Temperature

Plots of the anchorage-chair deflection data from the LVDTs for each of the six stay locations during the two monitoring periods are presented in Figures 16-21. The LVDT anchorage-chair deflection data also shows a trend with the external temperature data, but it exhibits an even greater response to the internal temperature (inside the anchorage end-cap). A temperature compensation calibration was used to correct the deviation in the response based on the change in internal temperature. While this did correct some of the deviation in response, the data still does not correlate to the external temperature as well as the CFCC load-cell force data or the FOS sensor data.

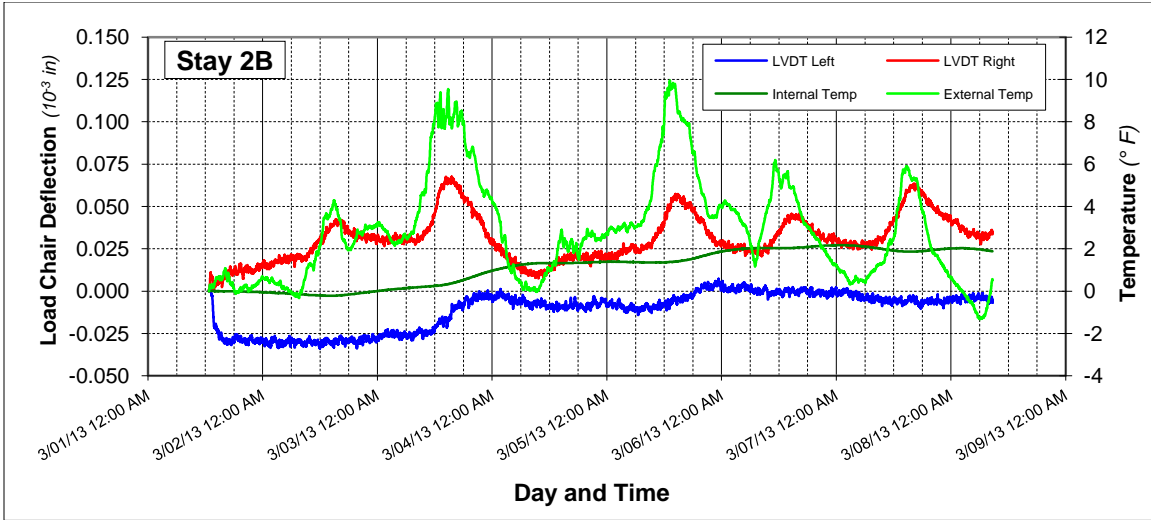


a)

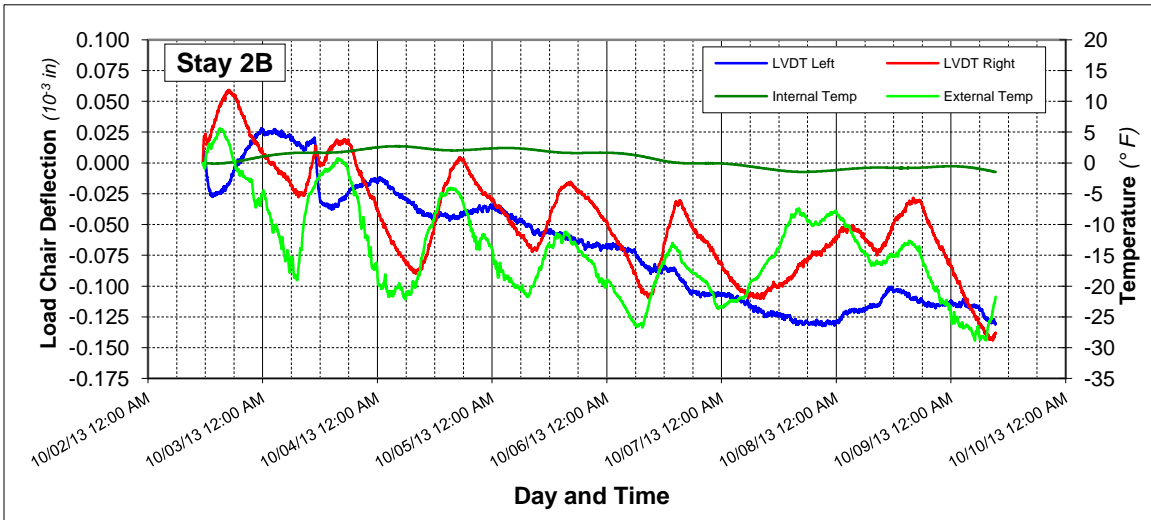


b)

**Figure 16. Anchorage-chair relative-deflection at Stay 2A during the continuous monitoring period in a) February 2013, and b) September 2013.**

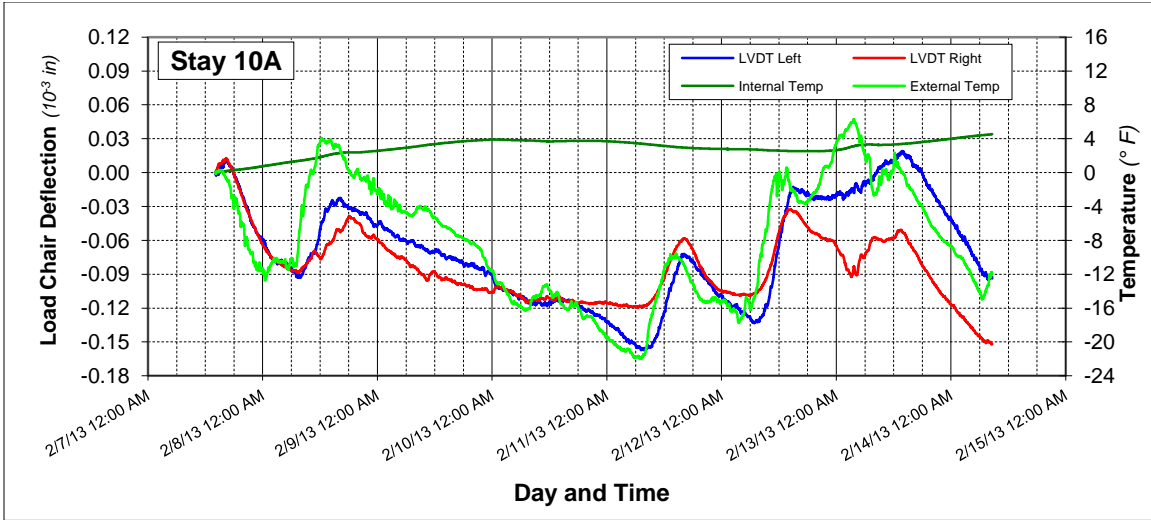


a)

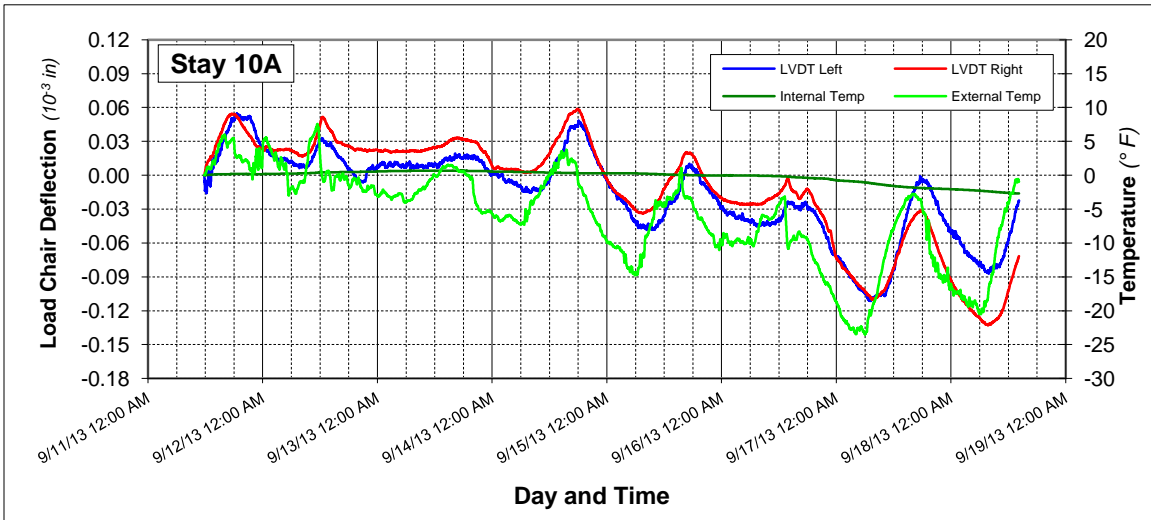


b)

**Figure 17. Anchorage-chair relative-deflection at Stay 2B during the continuous monitoring period in a) March 2013, and b) October 2013.**

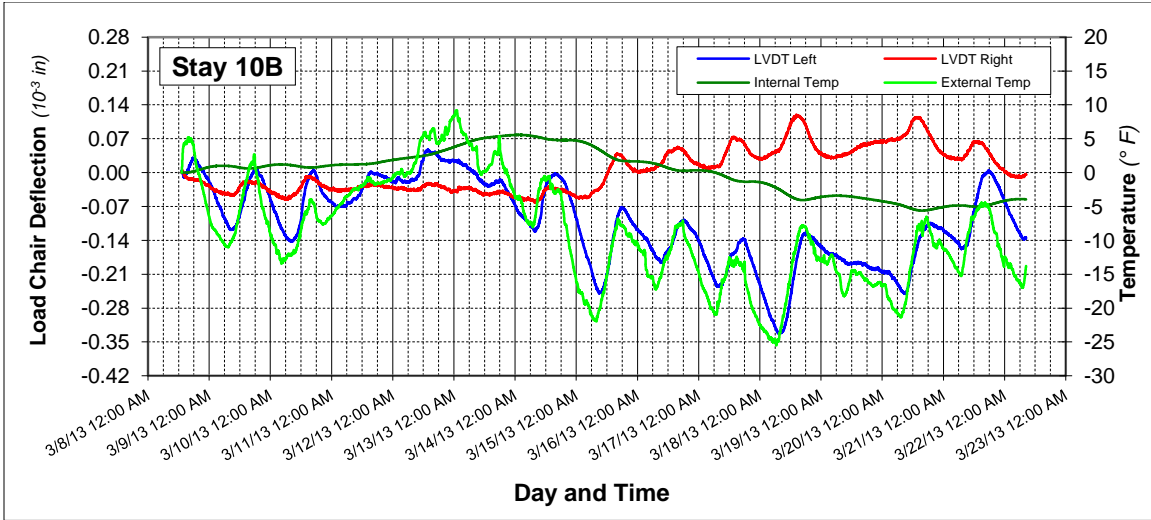


a)

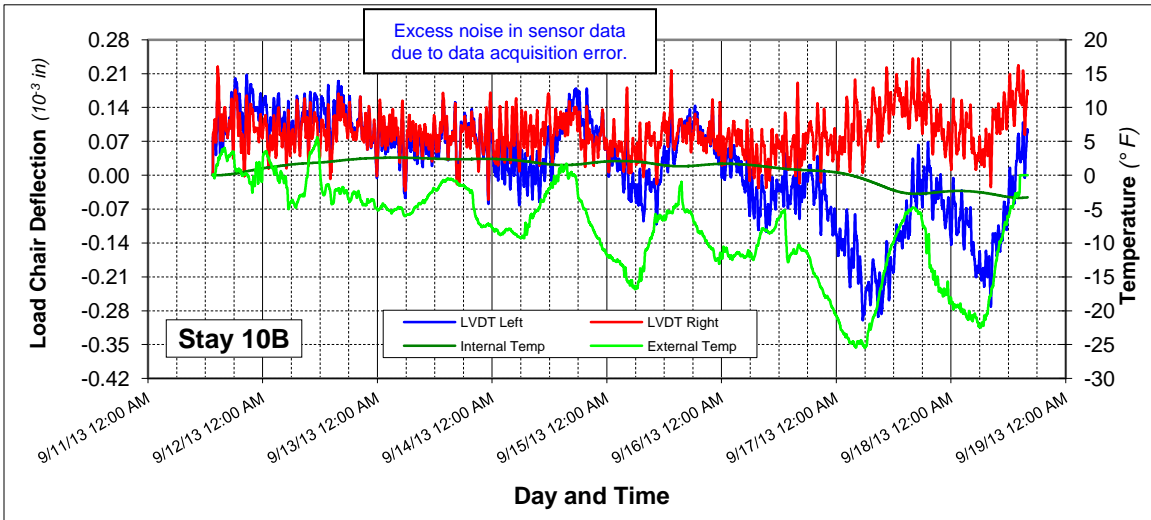


b)

**Figure 18. Anchorage-chair relative-deflection at Stay 10A during the continuous monitoring period in a) February 2013, and b) September 2013.**

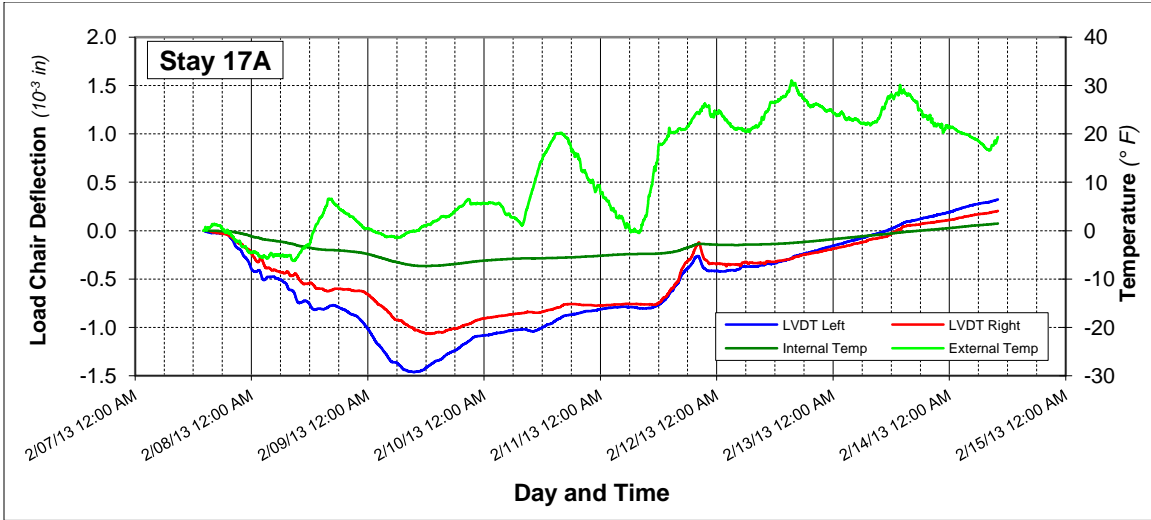


a)

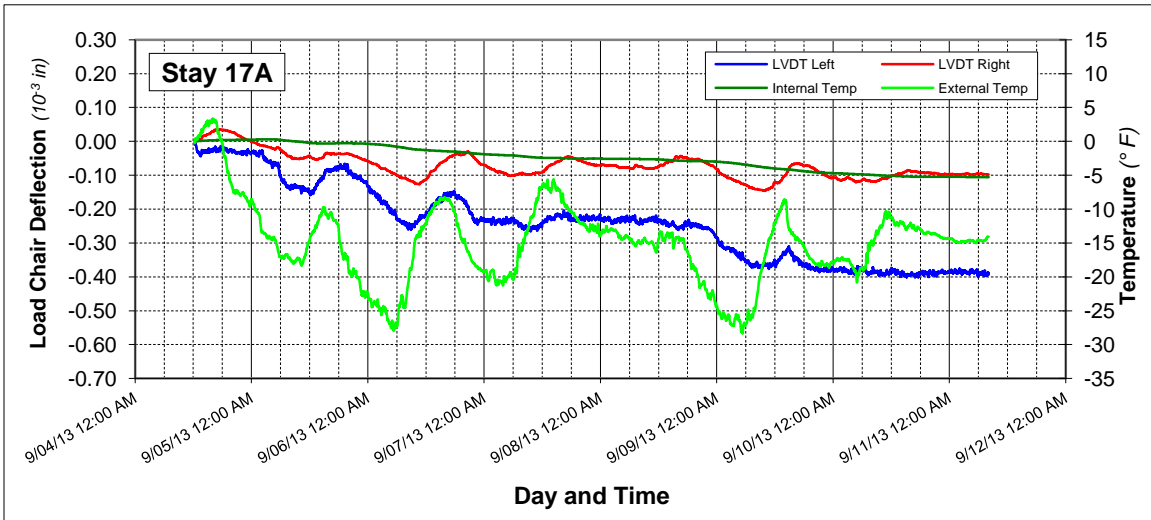


b)

**Figure 19. Anchorage-chair relative-deflection at Stay 10B during the continuous monitoring period in a) March 2013, and b) September 2013.**

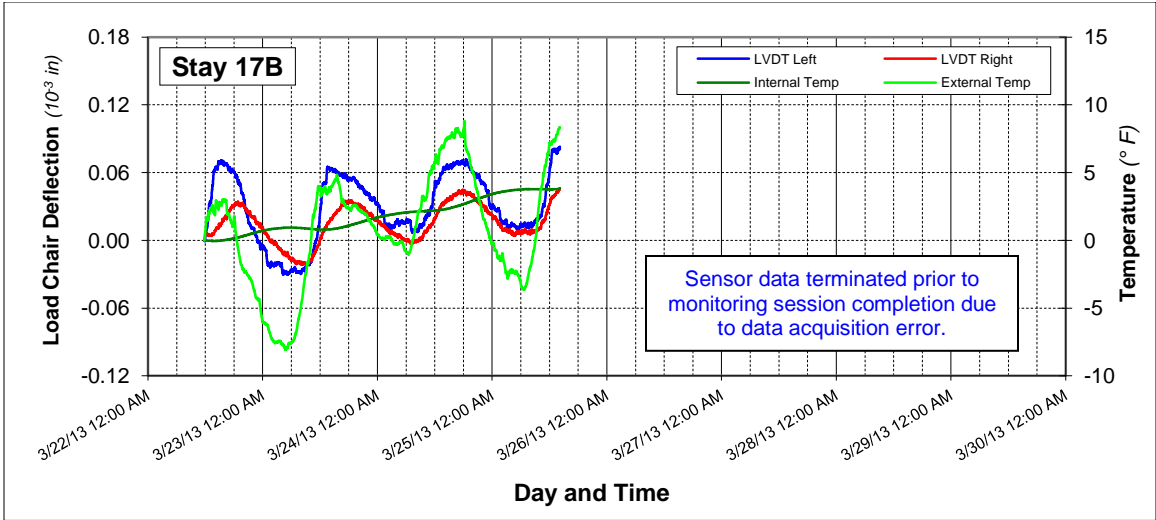


a)

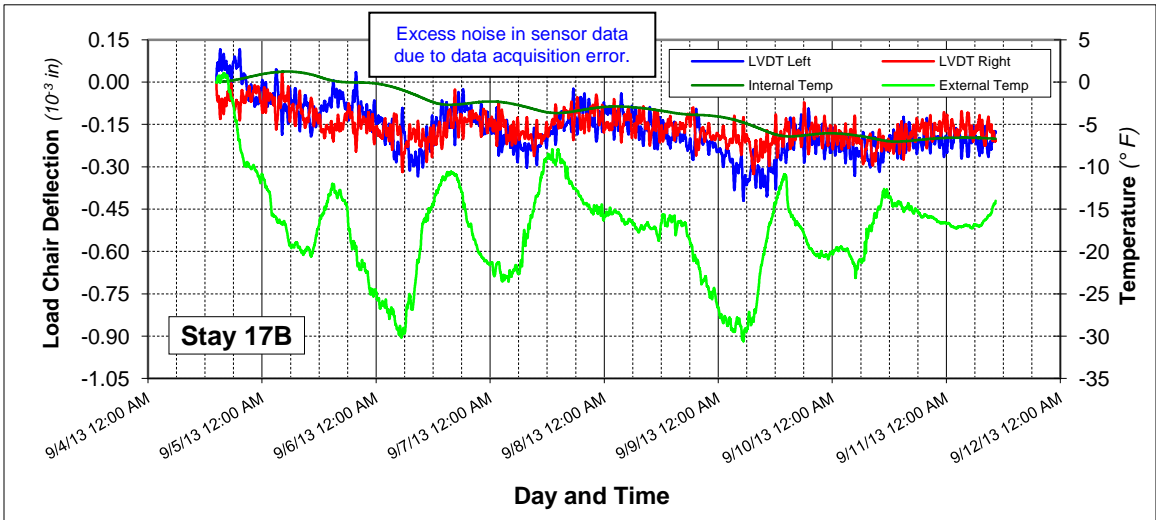


b)

**Figure 20. Anchorage-chair relative-deflection at Stay 17A during the continuous monitoring period in a) February 2013, and b) September 2013.**



a)



b)

**Figure 21. Anchorage-chair relative-deflection at Stay 17B during the continuous monitoring period in a) March 2013, and b) September 2013.**

#### 4. CFCC Force Compared to Fiber-Optic Sensor Strain

The FOS sensor system consists of two FOS sensors embedded in a thin composite sleeve. The sleeve is then attached to the CFCC strand in the stay anchorage via a combination of mechanical clamps and an adhesive.

The comparison of the relative CFCC force data obtained from the load-cells to the relative FOS sensor data obtained from the sleeves for the left and right cables at each stay anchorage location is presented in Figures 22-30. Since the intent of installing the FOS sensor sleeve system was to provide a redundant means of determining the force in the CFCC cables, it is necessary to be able to correlate the two sensors' responses.

There are two issues with the FOS sensor sleeve system. First, the original plan was to install the sleeves onto the CFCC strands during the CFCC strand tensioning process when the CFCC tension had reached 80% of its target load. It was discovered during the first sleeve installation that the twisting of the cable (during tensioning) would compromise the FOS sensor sleeve system. Therefore, this installation had to be abandoned and the sleeves had to be attached to the CFCC strands in their post-tensioned condition. The result of this is that the usable strain range of the sensors is limited. This can result in some nonlinear strain response, which means that the FOS sensor response will not correlate to the CFCC force response. The second issue is if the adhesive/clamping mechanism does not maintain a permanent bond to the CFCC strand, then the FOS sensor response will again not correlate to the CFCC force response. Some of the sensor data seem to correlate very well (Stay 10A in Figure 24) while others indicate a tendency to drift over time (Stays 2A & 2B in Figures 22 & 23). Monitoring data over longer periods of time will help determine if the FOS sleeves can maintain correlation to the force in the CFCC strands.

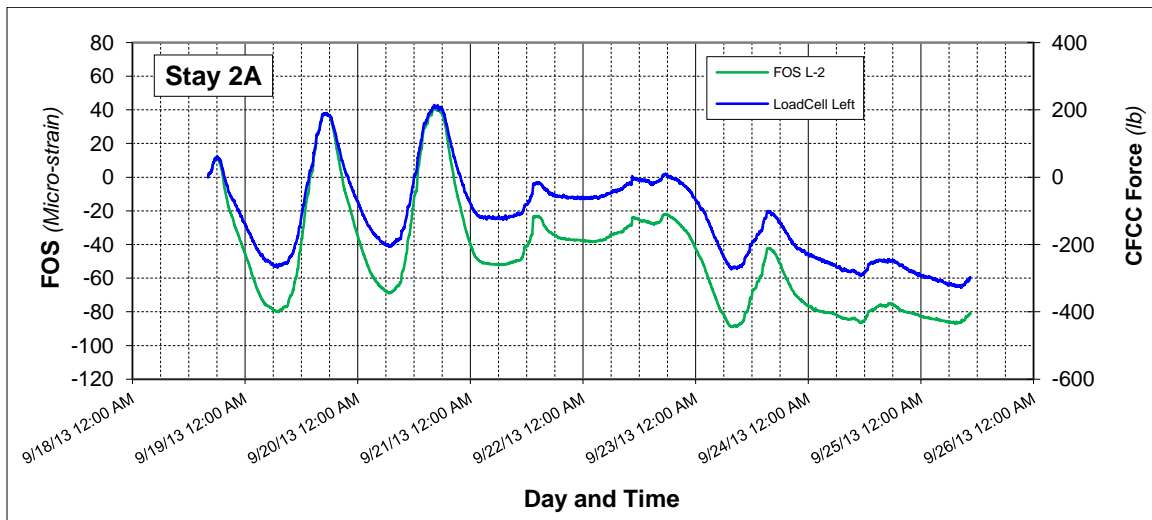
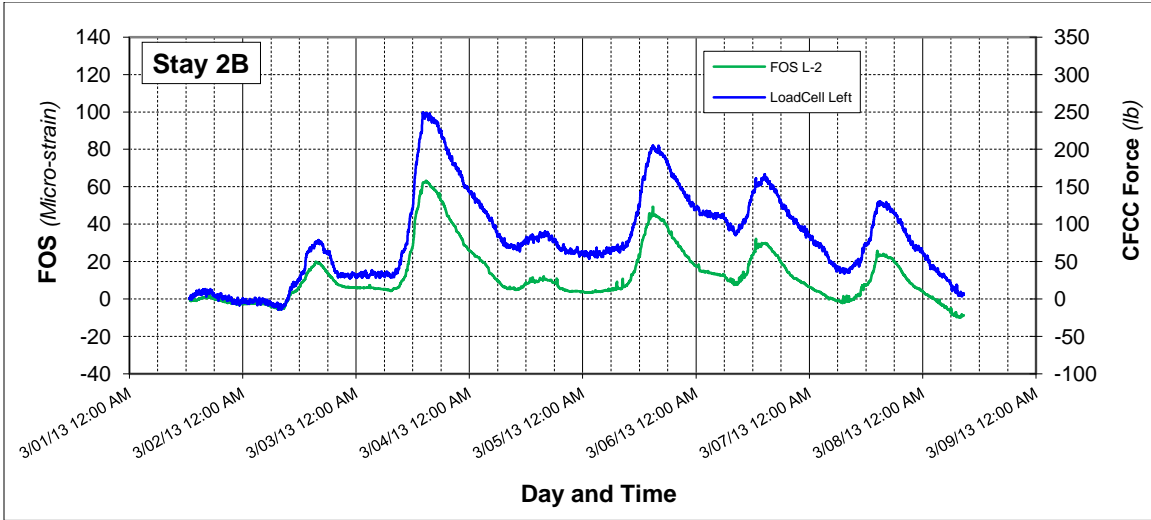
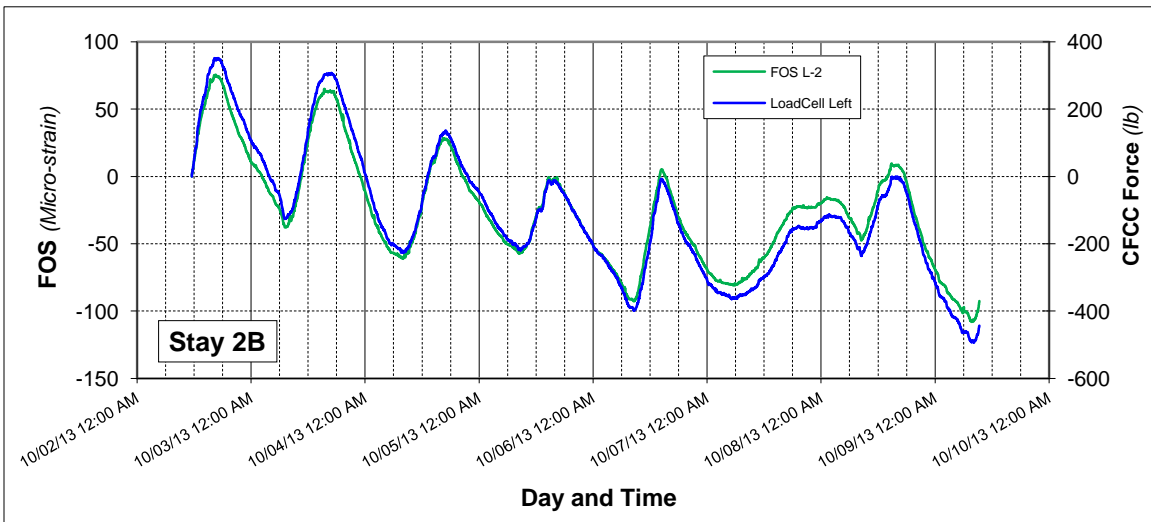


**Figure 22. CFCC force and FOS comparison at Stay 2A-Left during the continuous monitoring period in September 2013.**

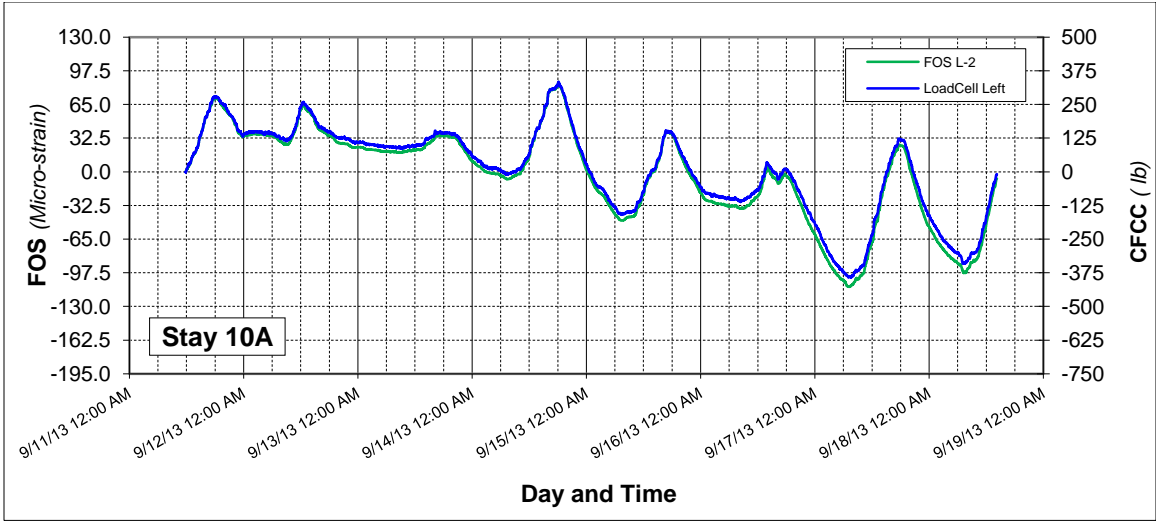


a)

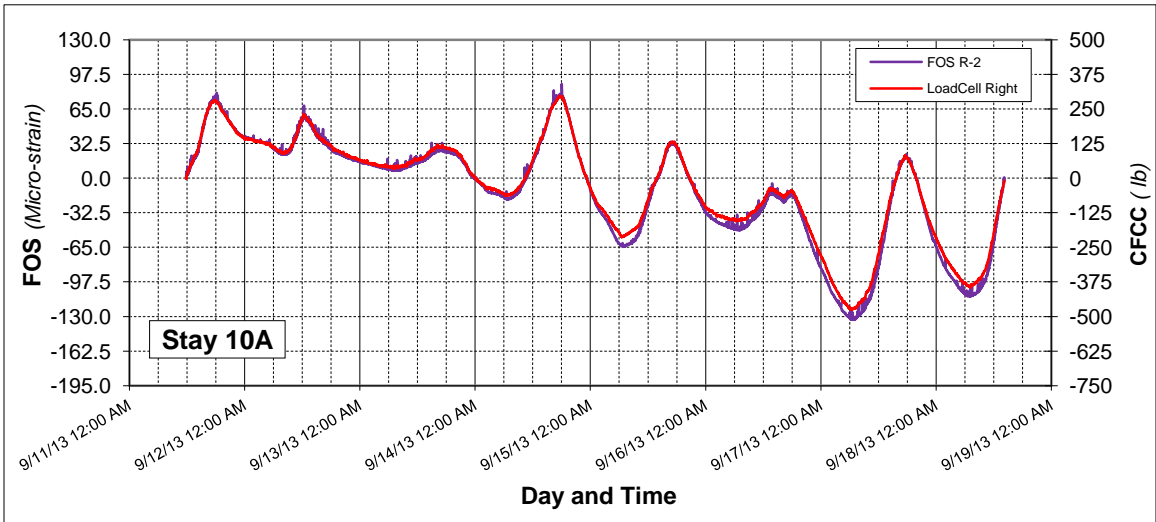


b)

**Figure 23. CFCC force and FOS comparison at Stay 2B-Left during the continuous monitoring period in a) March 2013, and b) October 2013.**

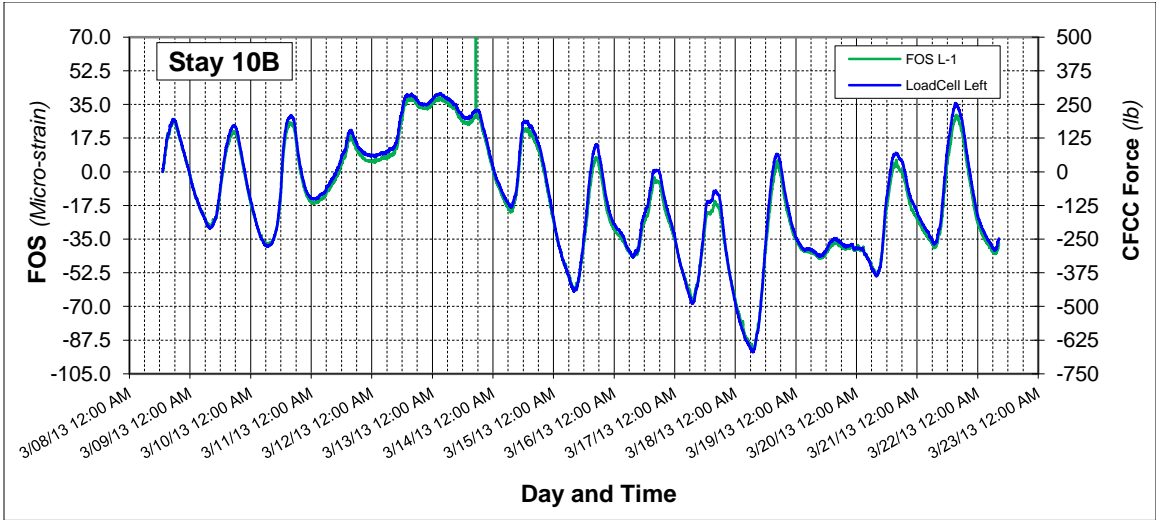


a)

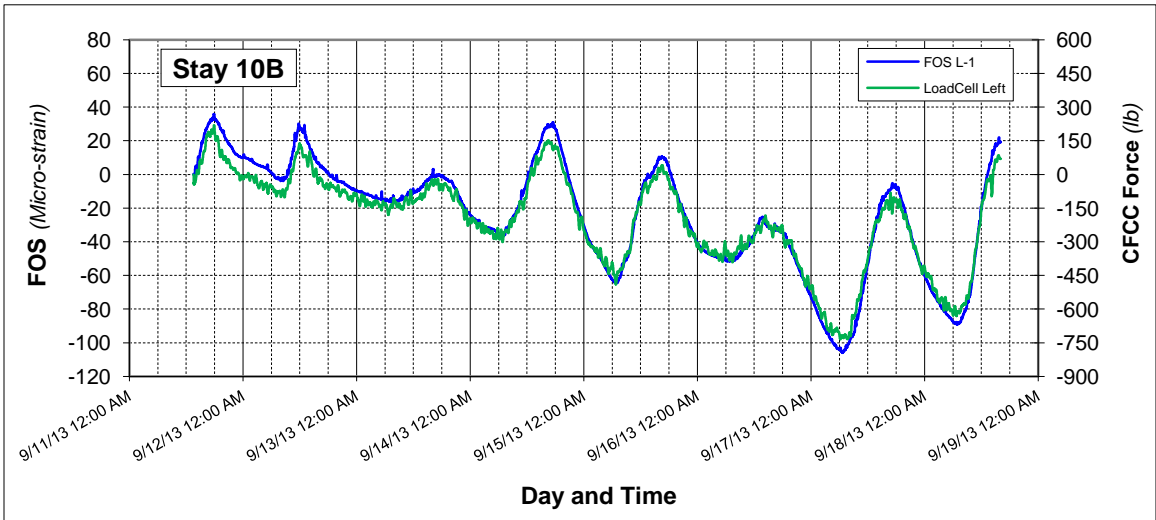


b)

**Figure 24. CFCC force and FOS comparison at Stay 10A during the September 2013 continuous monitoring period for a) Left cable and b) Right cable**

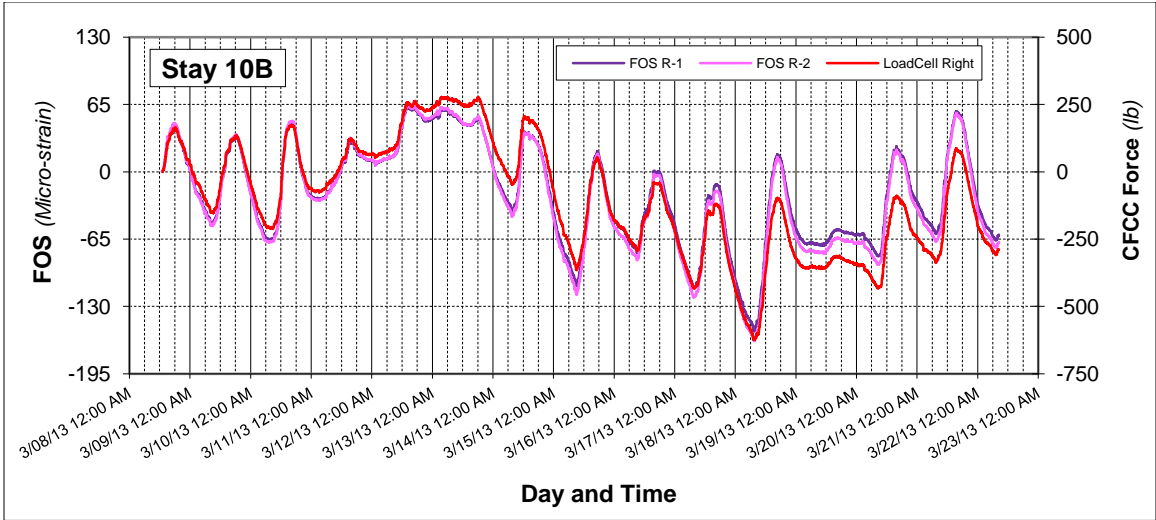


a)

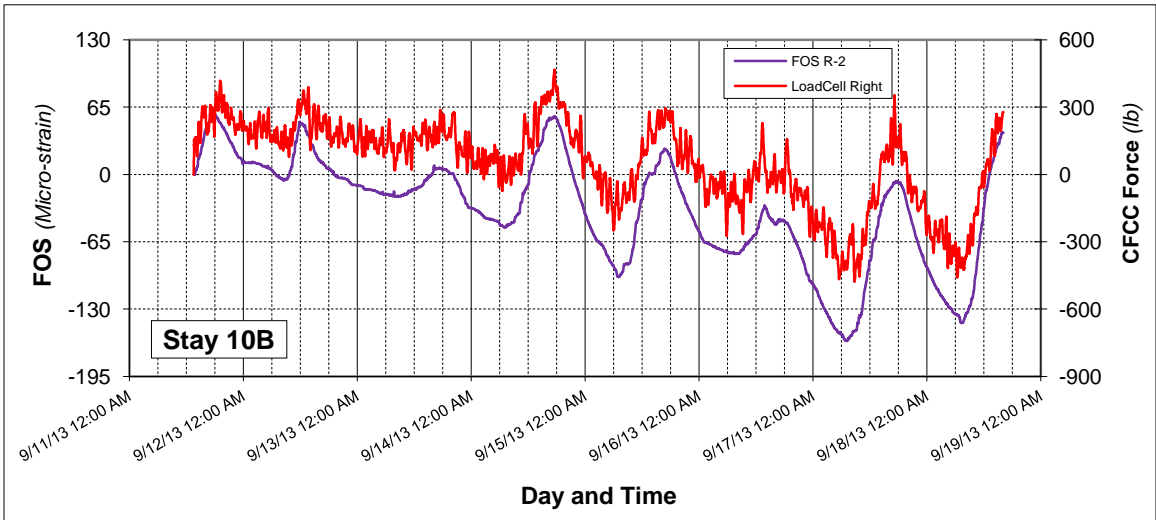


b)

**Figure 25. CFCC force and FOS comparison at Stay 10B-Left during the continuous monitoring period in a) March 2013, and b) September 2013.**



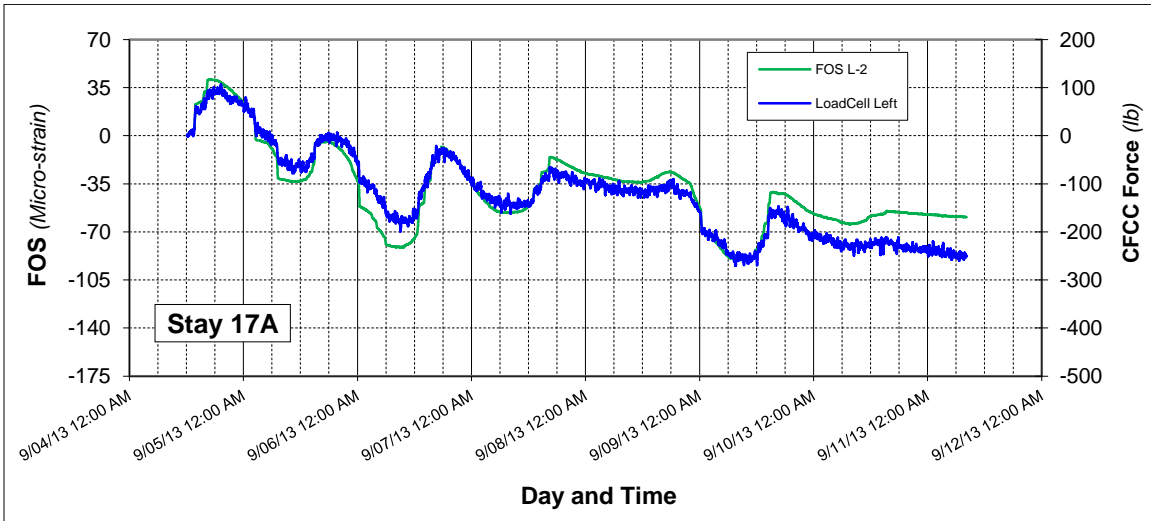
a)



b)

**Figure 26. CFCC force and FOS comparison at Stay 10B-Right during the continuous monitoring period in a) March 2013, and b) September 2013.**

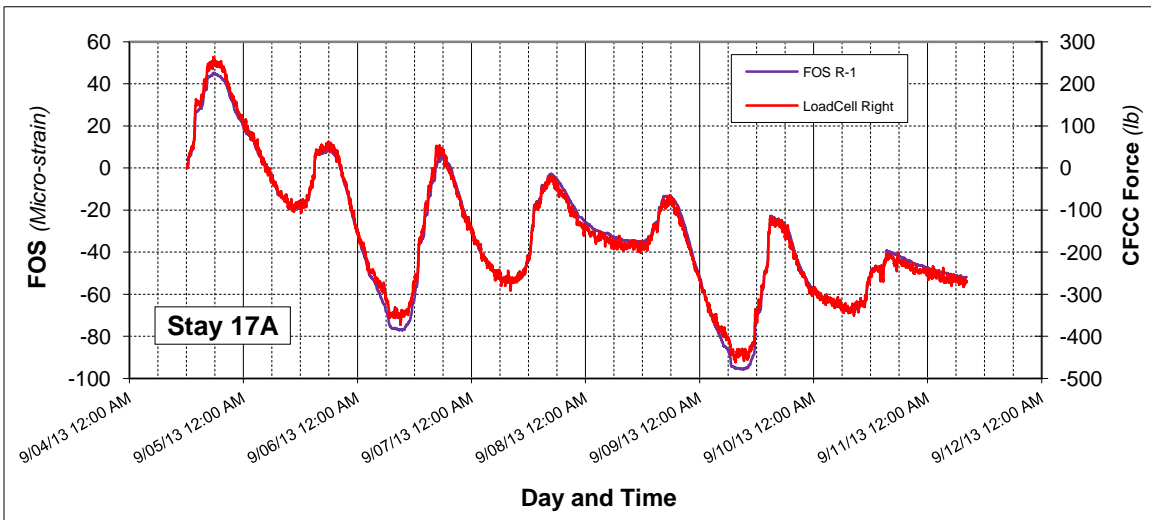
a) *THERE WAS NOT ANY FOS STRAIN DATA AVAILABLE AT THIS STAY LOCATION DURING THIS MONITORING CYCLE*



b)

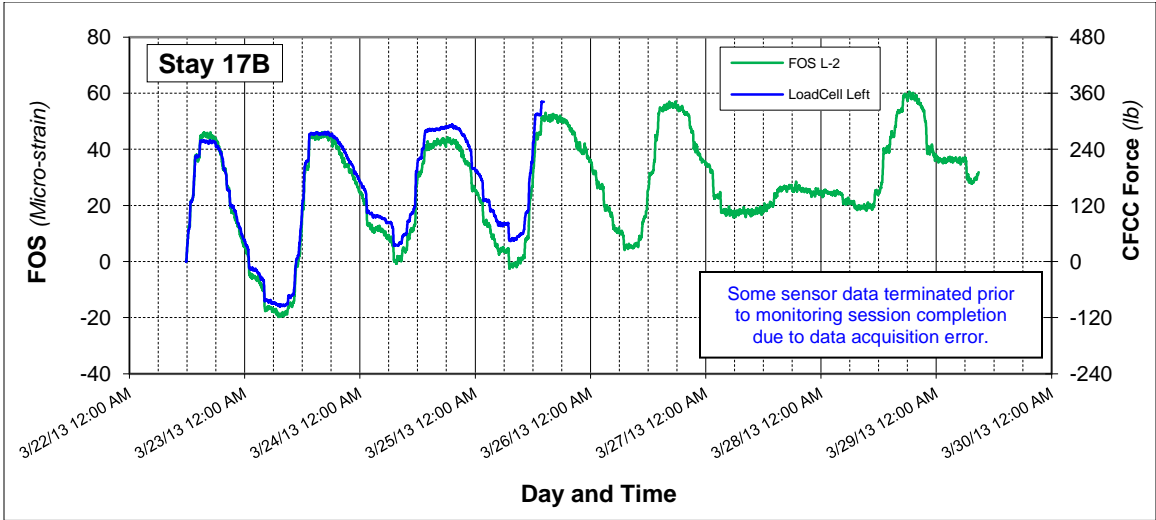
**Figure 27. CFCC force and FOS comparison at Stay 17A-Left during the continuous monitoring period in a) March 2013, and b) September 2013.**

a) *THERE WAS NOT ANY FOS STRAIN DATA AVAILABLE AT THIS STAY LOCATION DURING THIS MONITORING CYCLE*

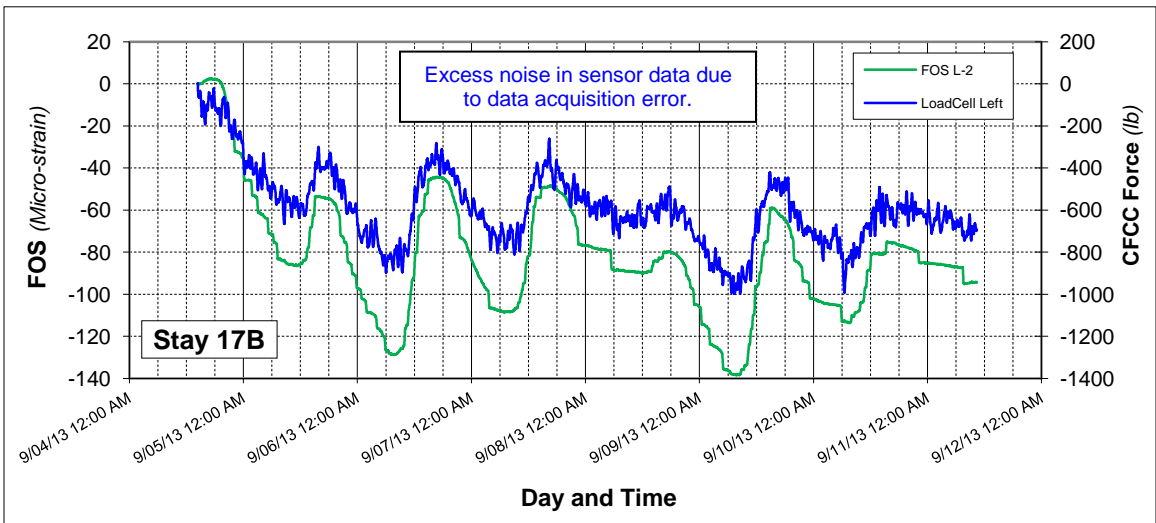


b)

**Figure 28. CFCC force and FOS comparison at Stay 17A-Right during the continuous monitoring period in a) March 2013, and b) September 2013.**

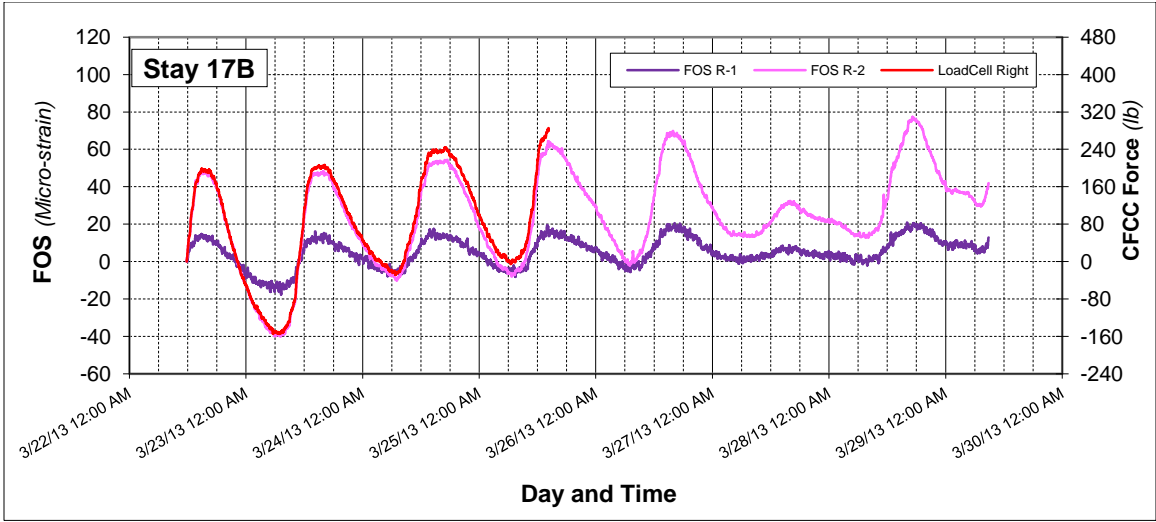


a)

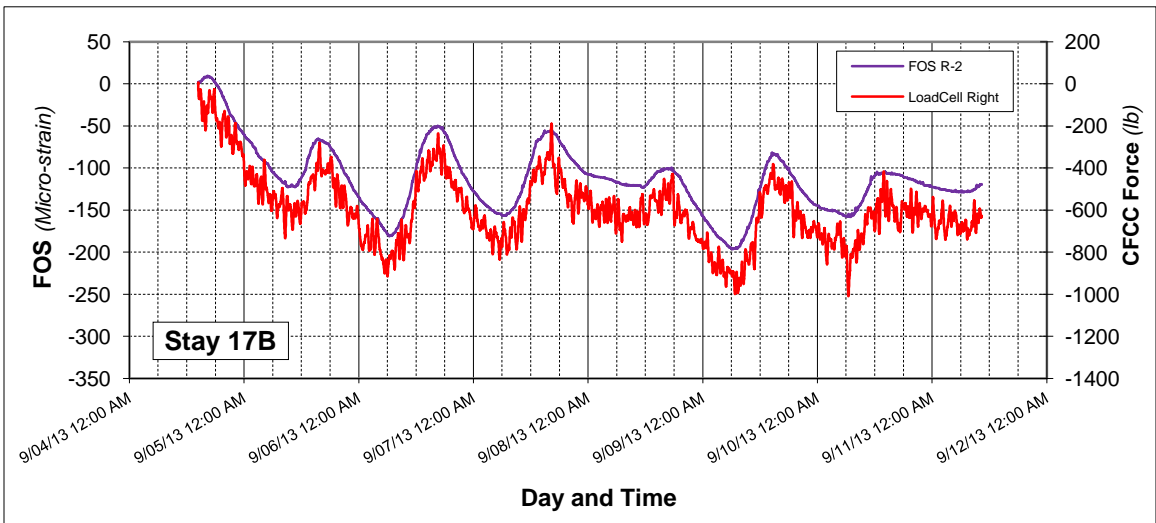


b)

**Figure 29. CFCC force and FOS comparison at Stay 17B-Left during the continuous monitoring period in a) March 2013, and b) September 2013.**



a)



b)

**Figure 30. CFCC force and FOS comparison at Stay 17B-Right during the continuous monitoring period in a) March 2013, and b) September 2013.**

## 5. CFCC Force Compared to LVDT Anchorage-Chair Deflection

The comparison of the relative CFCC force data obtained from the load-cells is compared to the relative anchorage-chair deflection data obtained from the LVDTs for the left and right cables at each stay anchorage location in Figures 31-42. Since the intent of installing the LVDT system was to provide a redundant means of determining the force in the CFCC cables, it is necessary to be able to correlate the two sensors' responses.

There are two issues that affect the LVDT sensor response. First, they are sensitive to their ambient temperature surroundings, which can be accounted for by monitoring the internal end-cap temperature and adjusting the response accordingly. This has been accounted for in the plots in Figures 31-42. Second, some of the LVDT support hardware is in contact with the endcap housing at some of the stay anchorage locations. This was a result of unanticipated clearance and tolerance issues between the anchorage-chairs and the endcaps. Unfortunately, the effect of this contact on the LVDT response has not been properly determined, which explains why some of the responses in the comparison plots do not correlate very well.

Additional data over longer periods of time will help determine the exact correlation of the two issues affecting the LVDT anchorage-chair deflection data. If a proper correlation cannot be determined through analysis of further data, it may be possible to modify the LVDT connecting hardware through the end-cap's access port.

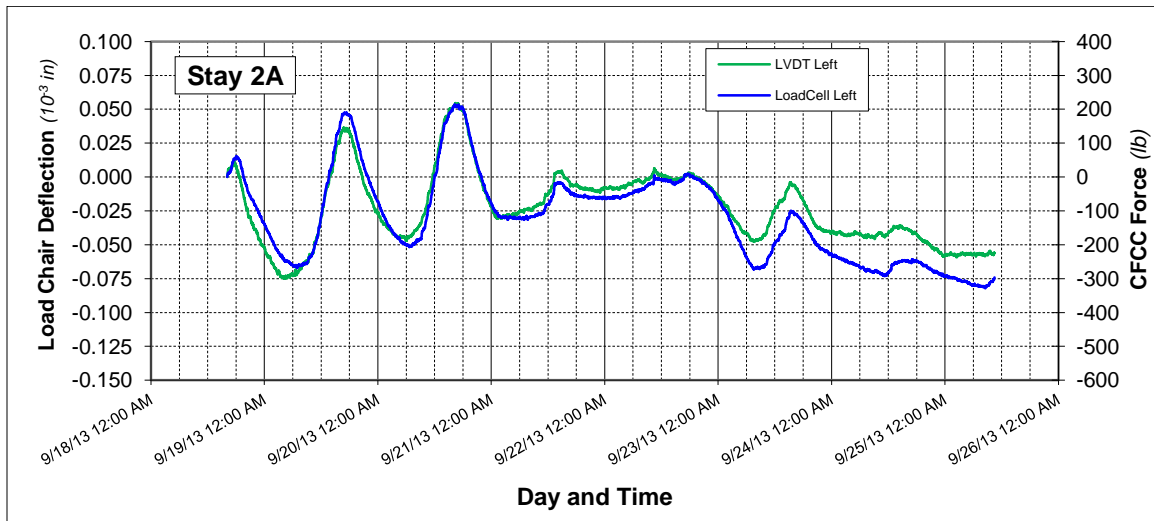


**Figure 31. CFCC force and anchorage-chair deflection comparison at Stay 2A-Left during the continuous monitoring period in September 2013.**

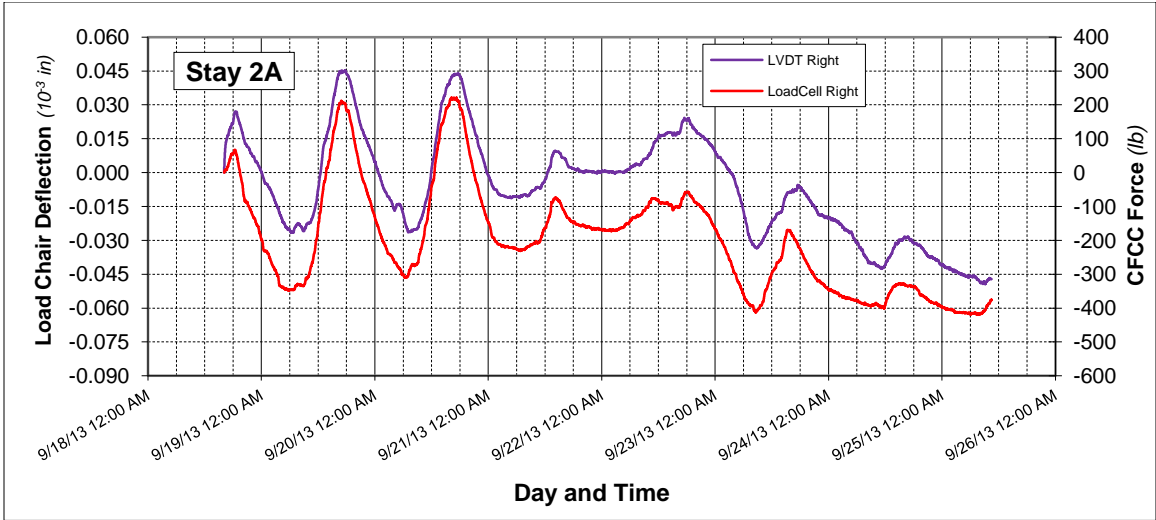


**Figure 32. CFCC force and anchorage-chair deflection comparison at Stay 2A-Right during the continuous monitoring period in September 2013.**

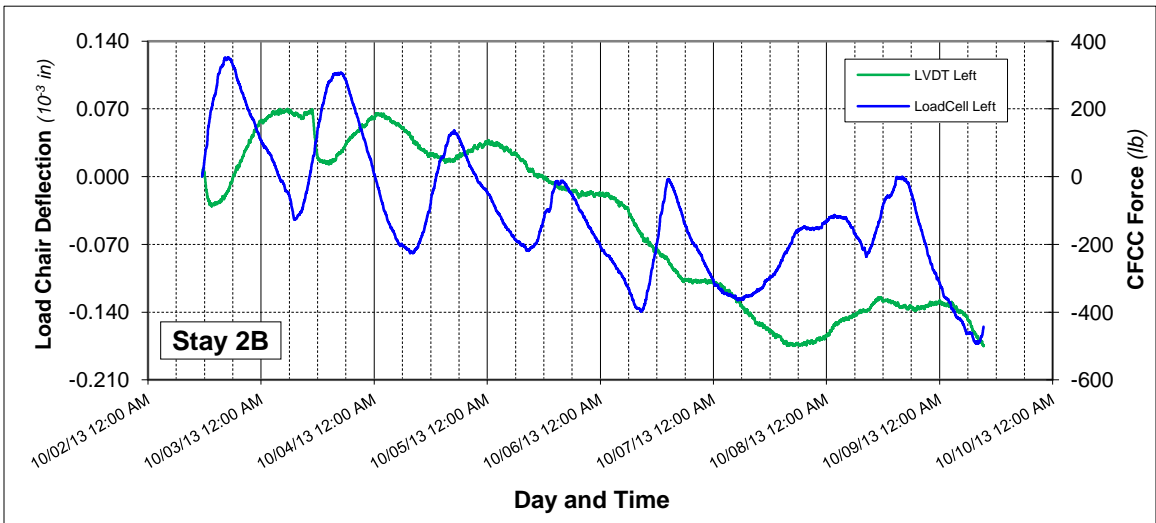
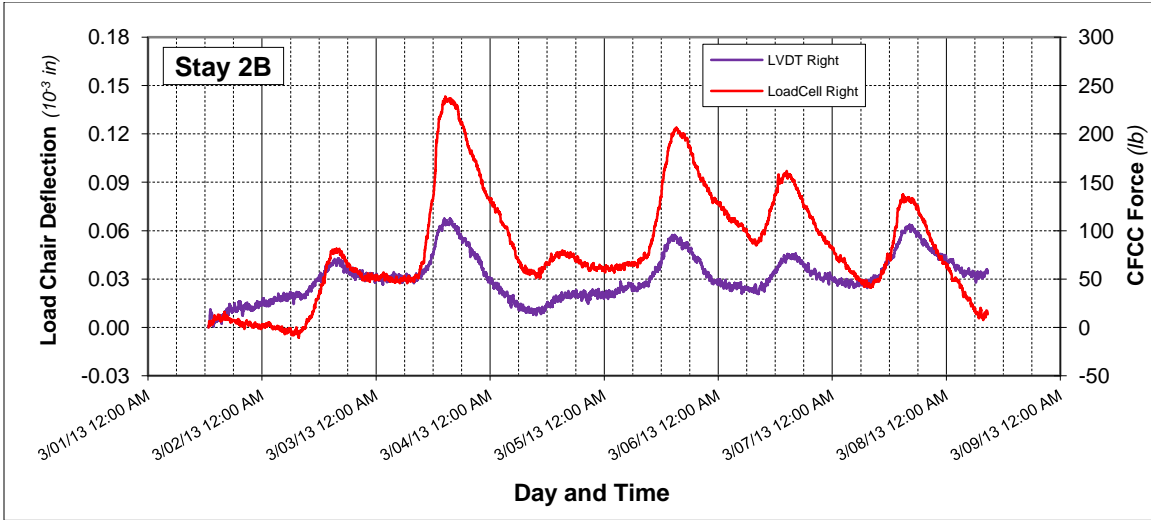
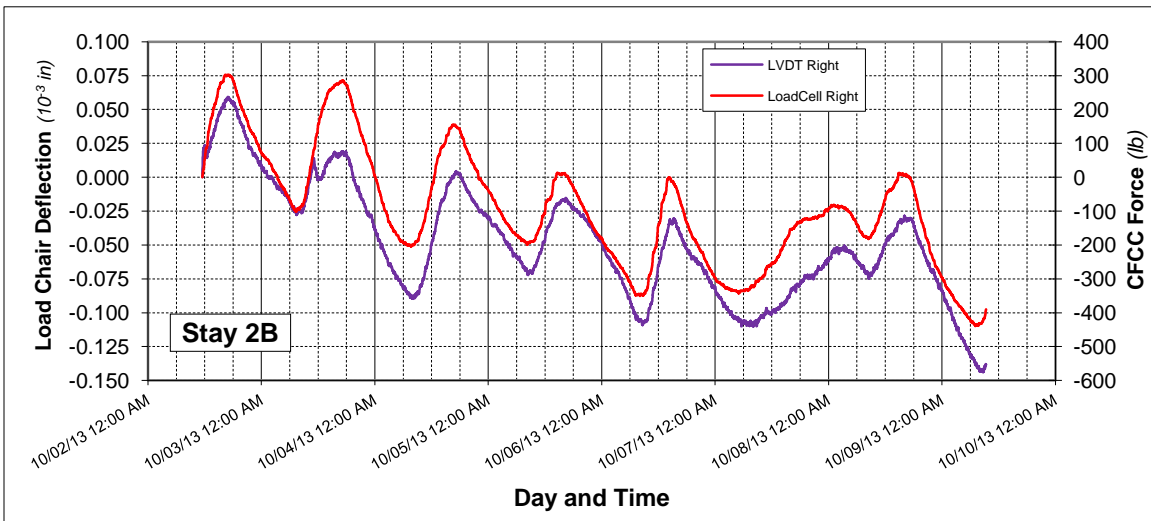


**Figure 33. CFCC force and anchorage-chair deflection comparison at Stay 2B-Left during the continuous monitoring period in October 2013.**

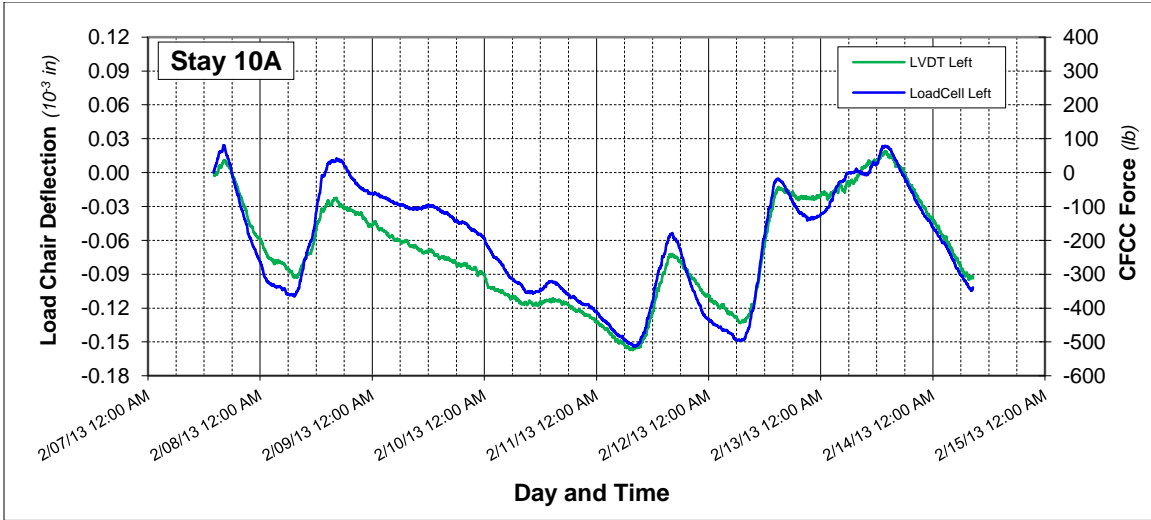


a)

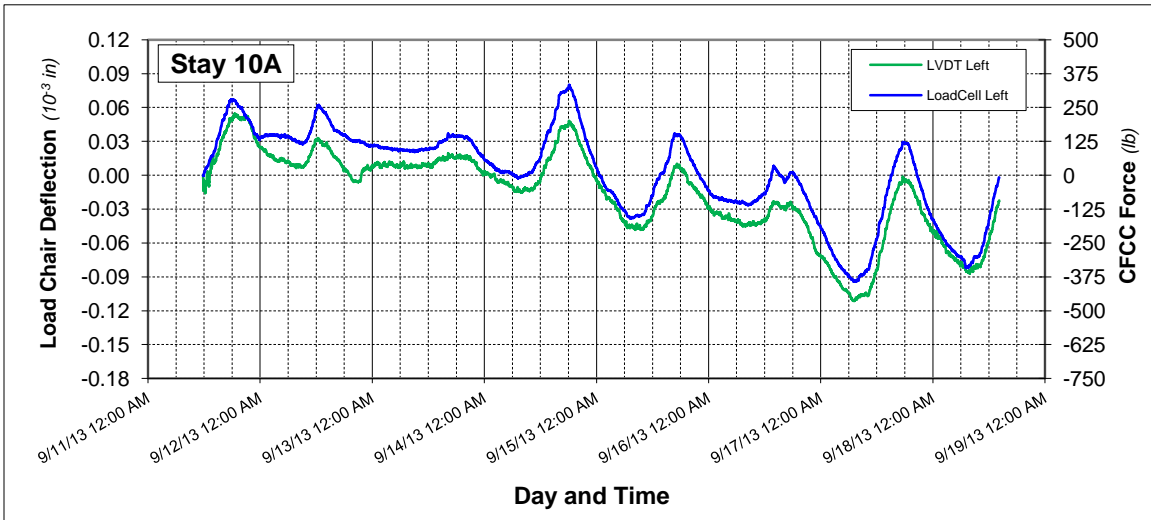


b)

**Figure 34. CFCC force and anchorage-chair deflection comparison at Stay 2B-Right during the continuous monitoring period in a) March 2013, and b) October 2013.**

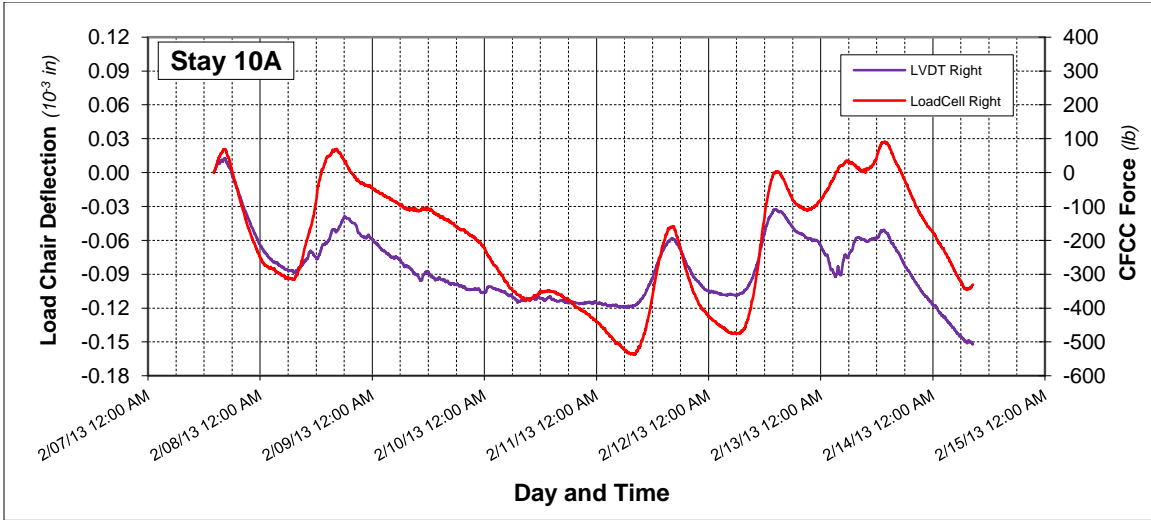


a)

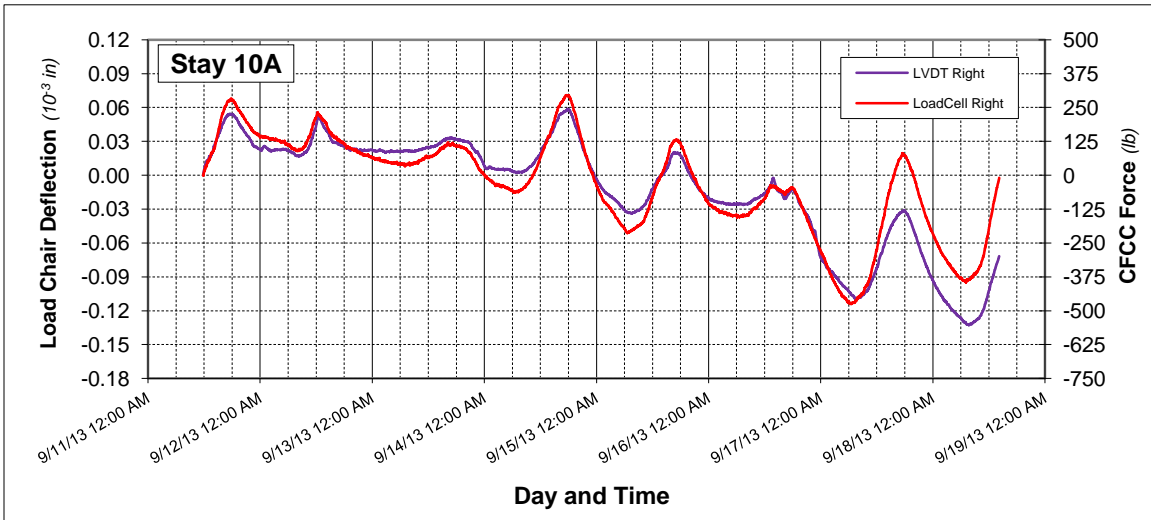


b)

**Figure 35. CFCC force and anchorage-chair deflection comparison at Stay 10A-Left during the continuous monitoring period a) February 2013, and b) September 2013.**

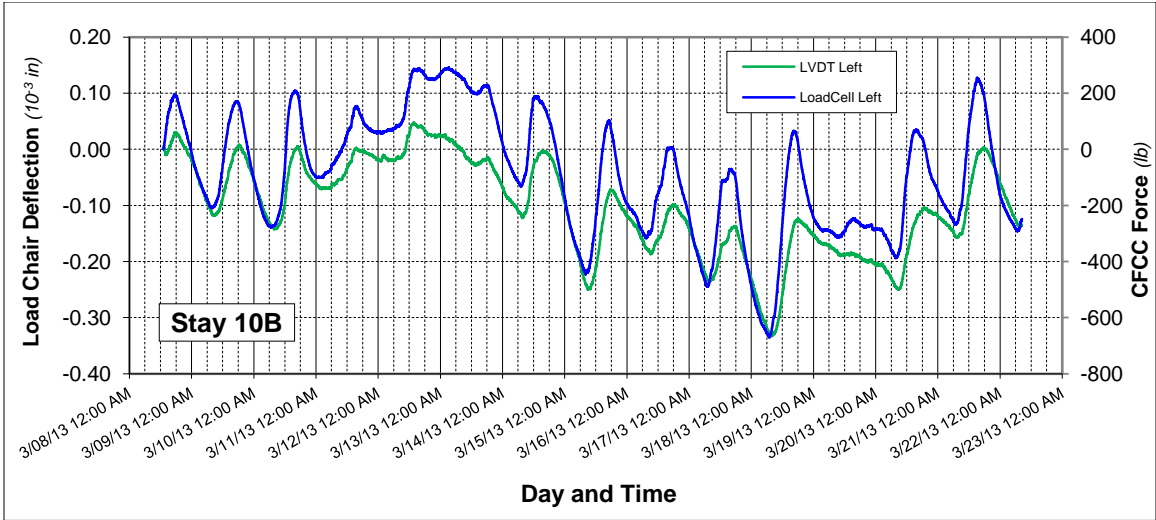


a)

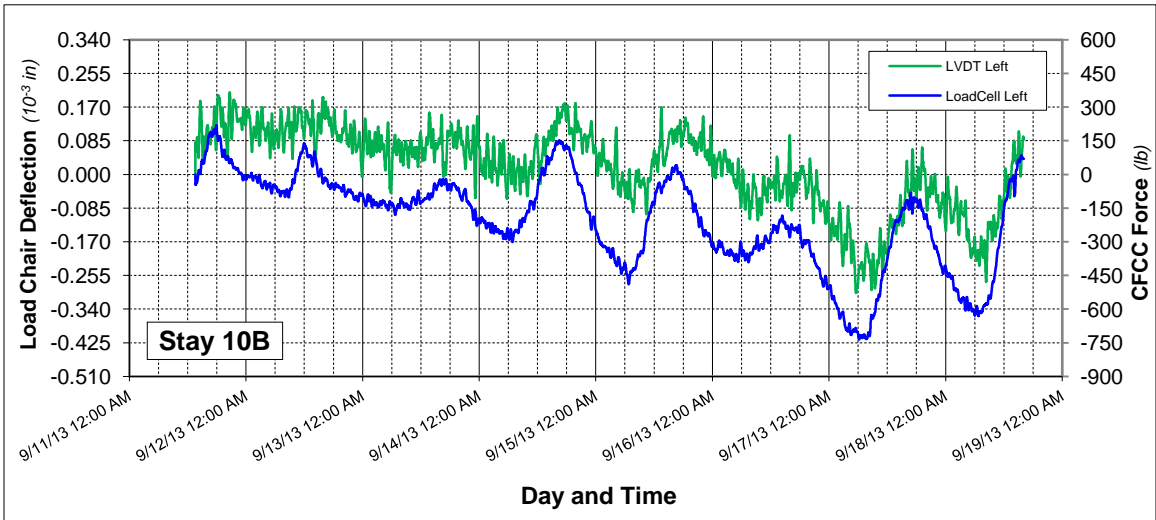


b)

**Figure 36. CFCC force and anchorage-chair deflection comparison at Stay 10A-Right during the continuous monitoring period a) February 2013, and b) September 2013.**

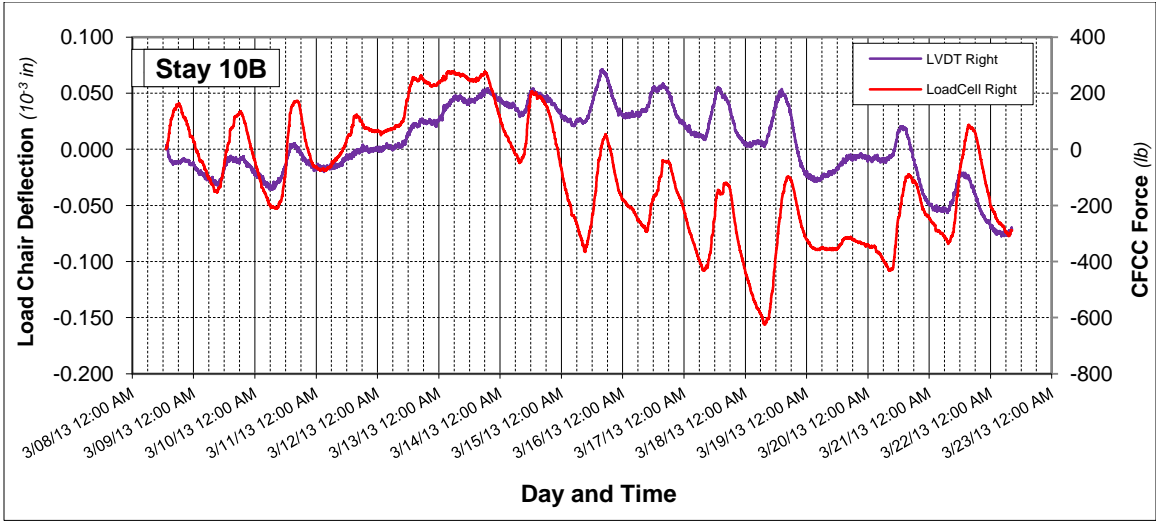


a)

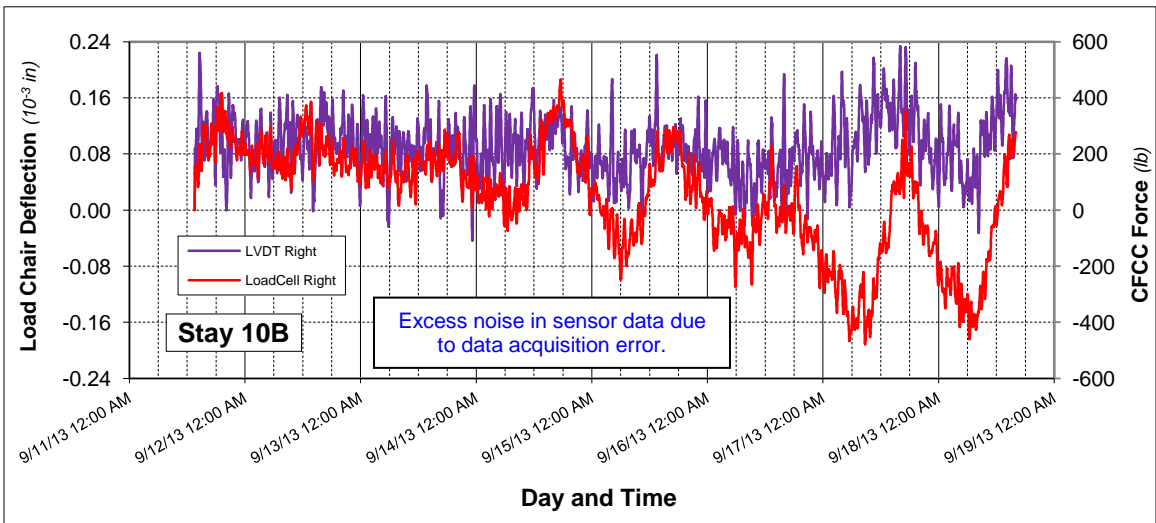


b)

**Figure 37. CFCC force and anchorage-chair deflection comparison at Stay 10B-Left during the continuous monitoring period in a) March 2013, and b) September 2013.**

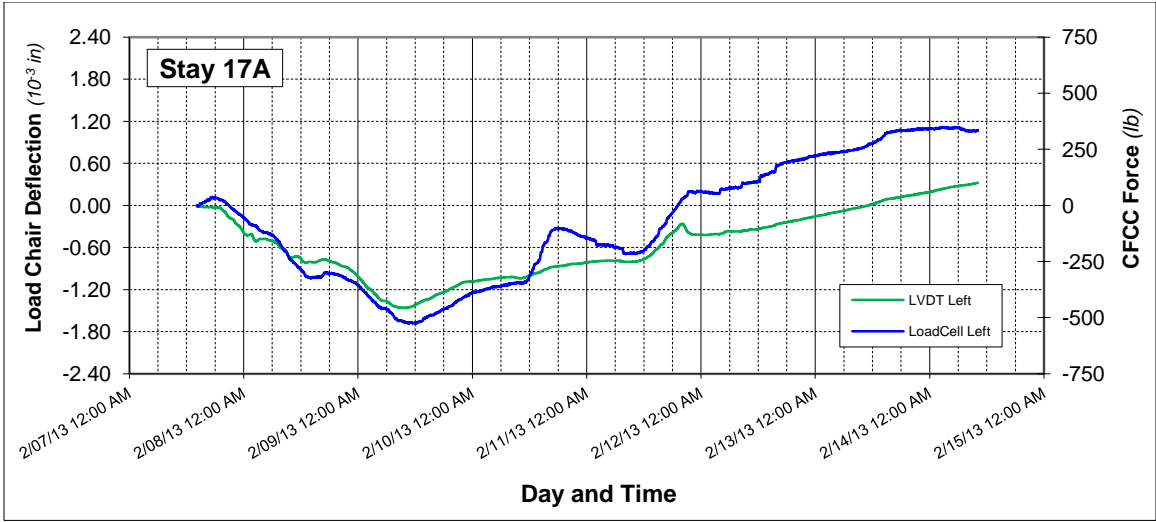


a)

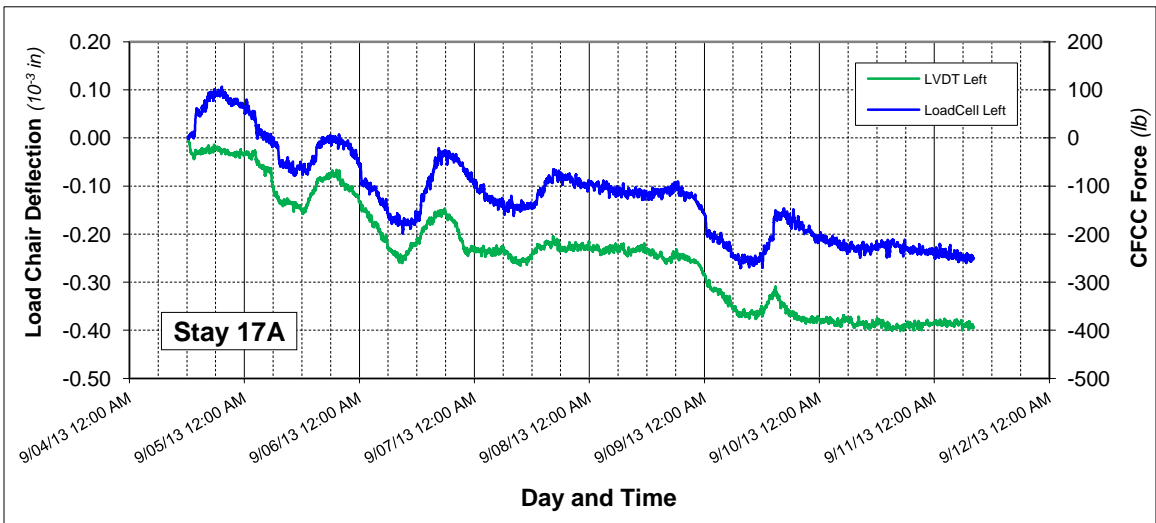


b)

**Figure 38. CFCC force and anchorage-chair deflection comparison at Stay 10B-Right during the continuous monitoring period in a) March 2013, and b) September 2013.**

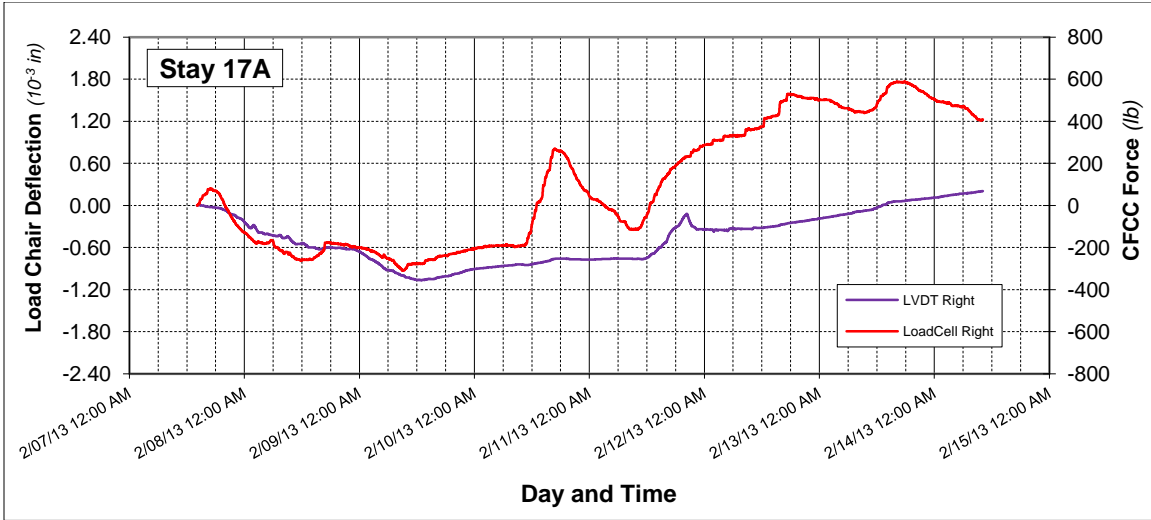


a)

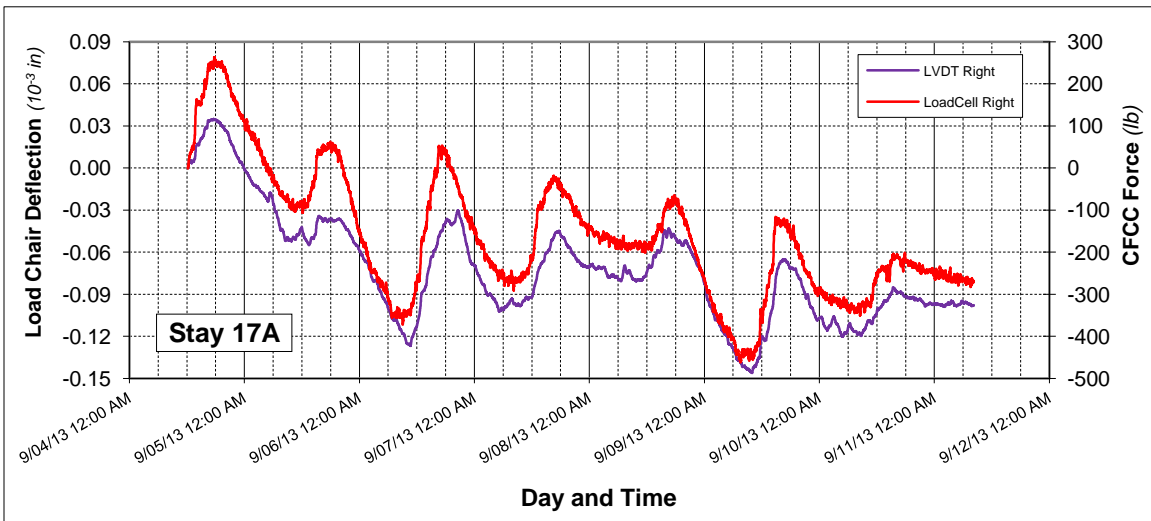


b)

**Figure 39. CFCC force and anchorage-chair deflection comparison at Stay 17A-Left during the continuous monitoring period a) February 2013, and b) September 2013.**

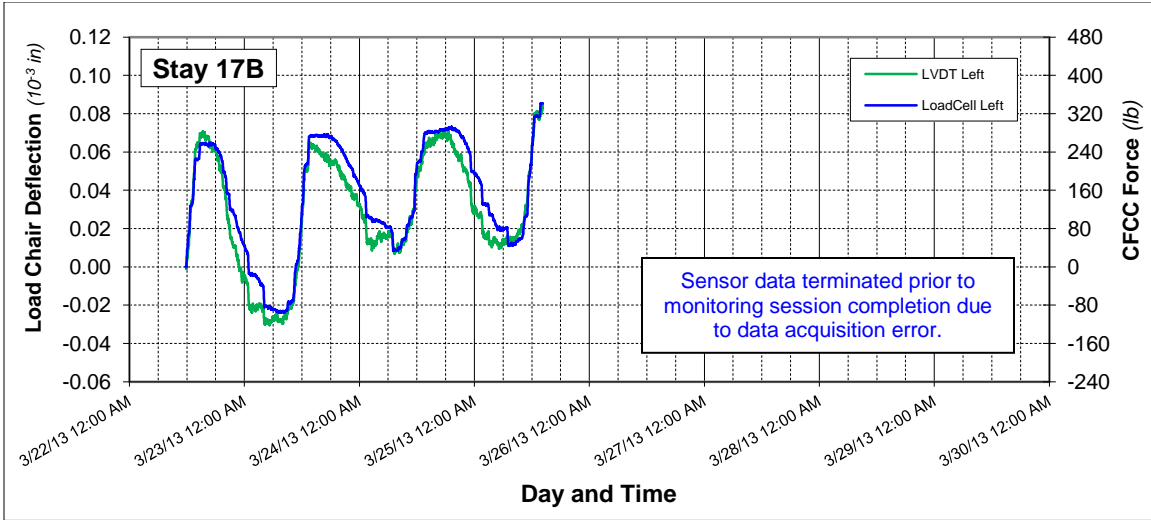


a)

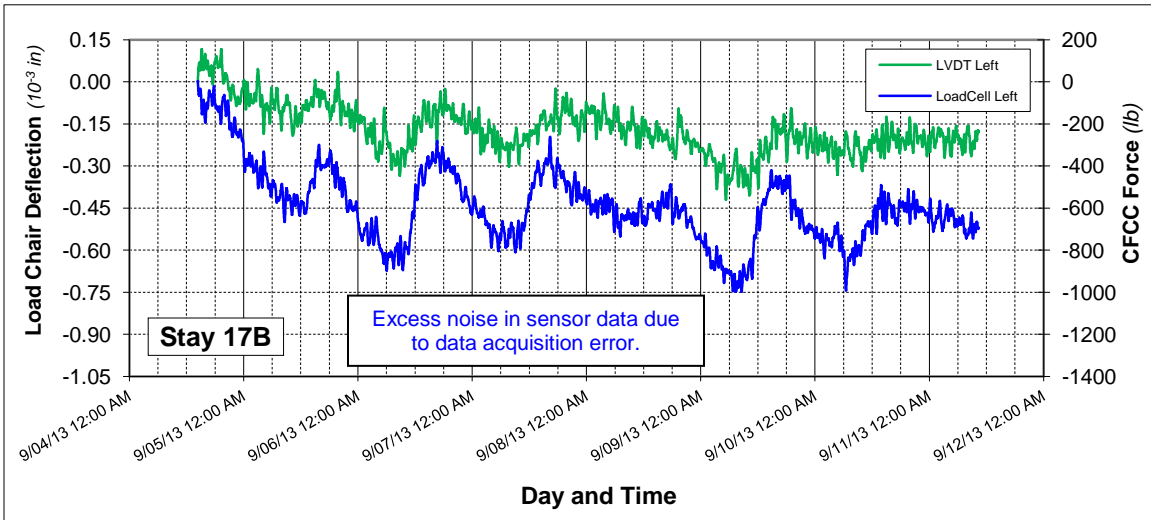


b)

**Figure 40. CFCC force and anchorage-chair deflection comparison at Stay 17A-Right during the continuous monitoring period a) February 2013, and b) September 2013.**

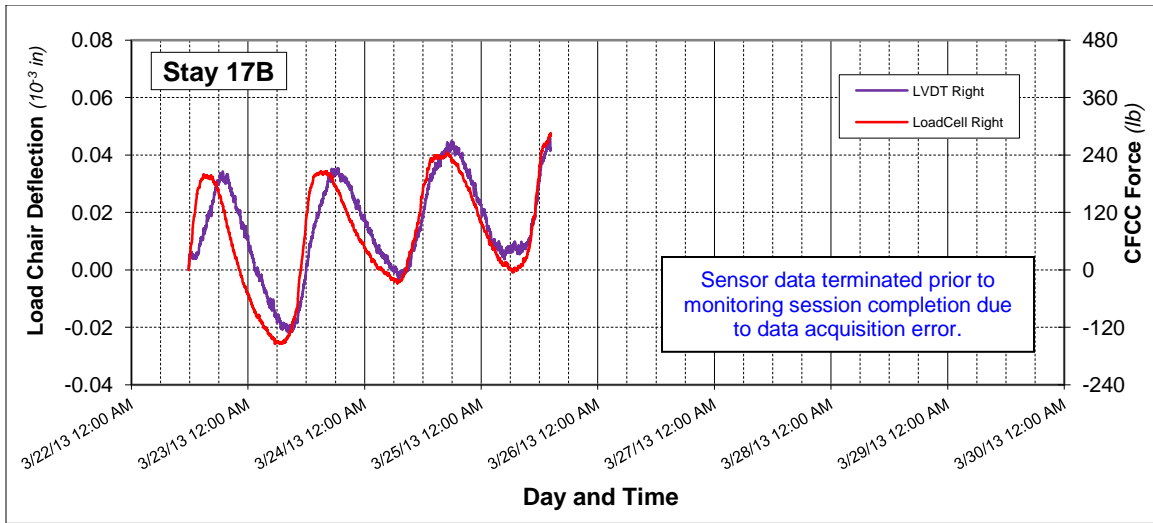


a)

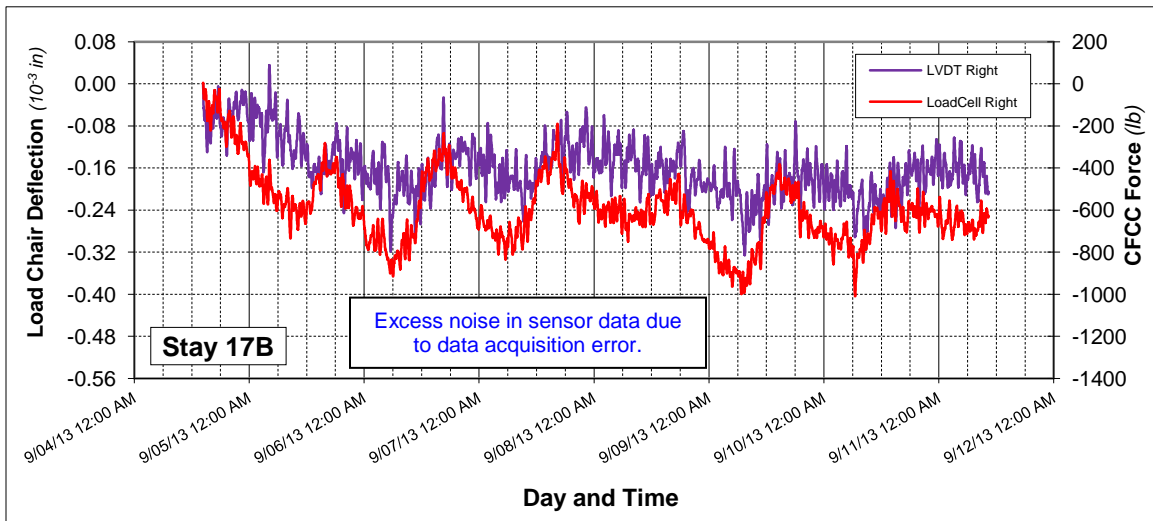


b)

**Figure 41. CFCC force and anchorage-chair deflection comparison at Stay 17B-Left during the continuous monitoring period in a) March 2013, and b) September 2013.**



a)



b)

**Figure 42. CFCC force and anchorage-chair deflection comparison at Stay 17B-Right during the continuous monitoring period in a) March 2013, and b) September 2013.**

## **CFCC System Modeling**

The analysis of the field monitoring data is ongoing. The intent is to establish a model that predicts the cable response based on changes in external temperature and other contributing factors.

During the Spring of 2014 a preliminary effort was conducted to analyze continuous CFCC structural health monitoring data collected over two separate time periods, and investigate the relationship between the external, ambient air temperature and the forces experienced by the CFCC strands, McDonald (2014). A numerical model of the heat transfer and thermoelasticity problems was developed and validated using sample monitoring data. The dynamic heat transfer problem was modeled using the lumped parameter method and various convection relationships sourced from Sucec (1985). The outer HDPE tube, steel cables, CFCC strands and internal air were treated as separate, lumped entities resulting in a system of coupled first-order differential heat transfer equations which were solved in time using MATLAB's ode23s routine. Once the temperatures were determined in the various elements, the forces in the cables were determined through the solution of a simple, quasi-static thermoelastic problem.

Upon completion of the numerical model, a numerical study was performed to assess the sensitivity of the CFCC forces to uncertainties in the thermal and mechanical property model inputs, and more importantly, to changes resulting from material or connection stress relaxation. The results of this exercise demonstrated that the dynamic CFCC forces are sensitive to selected heat transfer properties, and that the mean forces are significantly influenced by stress relaxation effects.

For the last part of the work, the numerical model was used to investigate CFCC force data collected during the continuous monitoring in 2008 and 2013 from the Penobscot Narrows Bridge at stay 10B. A fair correlation between experimental observations and numerical predictions was observed. The developed model predicted force amplitudes and phases reasonably well. This indicates that the transient heat transfer portion of the model properly accounts for the lag between changes in the ambient temperature and structural responses, and that the simplistic quasi-static thermoelastic formulation is sufficient to capture the bulk of the structural response.

For future work, the developed model can be used to track the relationship between CFCC force predictions and measurements to identify whether CFCC material or connection stress relaxation is present. The model will also be applied to the continuous monitoring data obtained from the other five stay locations. In addition, some experimental work may be conducted to verify some of the material and thermal parameters used in the thermoelastic model.

### **Task 3 – Feasibility study for connecting the instrumentation to the web based dry air monitoring system**

A bridge site visit by MaineDOT, UMaine and XL Mechanical and Energy Management Services (XL Mechanical) was conducted on April 12<sup>th</sup>, 2012. XL Mechanical had previously installed a dry-air online monitoring system at the site. The visit was intended to familiarize UMaine personnel with this system. The existing system is modular and expandable, which showed potential to allow integration with the CFCC structural monitoring system. The existing analog input modules are Honeywell XIO-8AI.

The intent of this task was to identify what instruments and sensors should be connected to provide online access to the structural monitoring data. Additionally, the existing dry air monitoring system was assessed for compatibility with the structural monitoring sensor system data. This task was limited to conducting a feasibility study, since the cost of implementation was unknown.

#### **Recommendations**

The existing Honeywell dry-air monitoring system has a resolution of  $\pm 10\text{mV}$ , while the existing CFCC monitoring data acquisition system has a resolution of  $\pm 0.33\text{ mV}$ . Based on this variation between the two systems and reduced response it would result in for the CFCC sensor system (by a factor of 30), it is recommended that the sensor system not use the existing Honeywell system as a means to implement the CFCC sensor system online.

The system that is proposed as an online health monitoring system for the CFCC strand instrumentation would use wireless communication to transmit the majority of the sensor data from each of the six stay anchorage locations to a central hub. The central hub will be located at the Prospect side tower. This reduces the cabling required for the long runs from each of the stay anchorage locations and maintains the integrity of the sensor data.

AC-to-DC power-supplies will be installed at each stay anchorage location to provide excitation voltage for the existing load-cells, anchorage-chair displacement sensors, and temperature sensors. The sensor output will be wired to a data acquisition module at the stay anchorage that will then transmit the sensor response back to the central hub via wireless transmission. System development is ongoing and onsite wireless system testing will be performed during the summer of 2015.

The FOS sensors require a special processing unit to provide the light source to power the sensors and to process the data. Installing such a unit at each stay anchorage location is cost prohibitive. Therefore, the FOS sensor system will require fiber-optic cabling to be run from the main hub to each of the stay locations. This is the most cost effective solution (based on current costs of the required system), since it will require a single processing unit. This unit can then interface with the system handling the wireless sensor data, or act as a stand-alone logging system that can be correlated to the remaining sensor data off-site at a later date.

## References

Berube, K.A., Lopez-Anido, R.A., and Caccese, V., (2008a). “Integrated Monitoring System for Carbon Composite Strands in the Penobscot-Narrows Cable-Stayed Bridge,” Transportation Research Record: Journal of the Transportation Research Board, No. 2050, pp. 177–186.

Berube, K.A., and Lopez-Anido, R.A., and Caccese, V., (2008b). “Initial Data Analysis of a Structural Health Monitoring System for Carbon Fiber Composite Strands in a Cable Stayed Bridge,” 25<sup>th</sup> Int. Bridge Conf., Paper IBC-08-17, 9 pp., Jun. 2–4, Pittsburgh, PA.

Lopez-Anido, R.A., Caccese, V., and Berube, K.A., (2009) “Integrated Monitoring System for CFCC Cables in the Penobscot Narrows Bridge,” AEWG Report 10-03, University of Maine, Orono, ME. 148 pp.

McDonald, K., (2014), Numerical Model for Predicting CFCC Forces in a Cable-Stayed Bridge, Griffith University & Advanced Structures and Composites Center Report, 73pp.

Sucec, J. (1985). Heat Transfer. WM. C. Brown Publishers. Dubuque, Iowa.